

Structure of Periodic Orbit Families in the Hill Restricted 4-Body Problem

Gavin M. Brown^{1*}, Luke T. Peterson¹, Damennick B. Henry¹,
Daniel J. Scheeres¹

¹Ann and H.J. Smead Aerospace Engineering Sciences, University of Colorado
Boulder, CO, USA.

*Corresponding author(s). E-mail(s): gavin.m.brown@colorado.edu;
Contributing authors: Luke.Peterson@colorado.edu;
Damennick.Henry@colorado.edu; scheeres@colorado.edu;

Abstract

The Hill Restricted 4-Body Problem (HR4BP) is a coherent time-periodic model that can be used to represent motion in the Sun-Earth-Moon (SEM) system. Periodic orbits were computed in this model to better understand the periodic orbit family structures that exist in these types of systems. First, periodic orbits in the Circular Restricted 3-Body Problem (CR3BP) representation of the Earth-Moon (EM) system were identified. A Melnikov-type function was used to identify a set of candidate points on the EM CR3BP periodic orbits to start a continuation algorithm. A pseudo-arclength continuation scheme was then used to obtain the corresponding periodic orbit families in the HR4BP when including the effect of the Sun. Bifurcation points were identified in the computed families to obtain additional orbit families.

Keywords: Periodic orbits, Bifurcations, Three-Body Problems, Melnikov Function, Sun-Earth-Moon System

Contents

1	Introduction	3
2	Problem Formulation	3
2.1	Formulation of the HR4BP	3
2.2	Melnikov Theory	5
3	Methodology	6
3.1	Expanding the HR4BP Equations of Motion	6
3.2	Behavior of the HR4BP Melnikov Function	7
3.3	Generating HR4BP Periodic Orbit Families	9
4	Periodic Orbits	10
4.1	Families from EM Libration Points and Associated Periodic Orbits	11
5	Conclusion	14
A	HR4BP Equations of Motion	15
B	Melnikov Theory Applications with the HR4BP	17
B.1	Introduction to Melnikov Theory	17
B.2	Manipulating the HR4BP Equations of Motion	20

1 Introduction

Cislunar space is the operating environment for many current and future spacecraft missions. It is the target of NASA’s planned Gateway, a crewed space station in orbit near the Moon, and the focus of many other NASA objectives [1, 2]. The Circular Restricted 3-Body Problem (CR3BP) is one of the most basic dynamical models we have to represent motion in cislunar space. There are several dynamical models that seek to present a more realistic representation of motion in cislunar space than the CR3BP. The Elliptic Restricted 3-Body Problem (ER3BP) includes the effect of the eccentricity of the two primaries’ orbit [3–5]. Other models also attempt to account for the effect of the Sun on the motion of a spacecraft in the Earth-Moon (EM) system. One such model is the Bicircular Restricted 4-Body Problem (BCP), which is incoherent as it does not account for the effect of the Sun on the Earth or the Moon [6–8]. In addition, there is no accurate dynamical equivalent to L_2 which is one major drawback of the BCP [9]. Periodic orbits in the BCP corresponding to the CR3BP triangular points have been computed previously [10], as have families of periodic orbits [11] and quasi-periodic orbits [12, 13]. Unlike the BCP, the Quasi-Bicircular Model (QBCP) accounts for the effect of the Sun on the Earth and Moon by modeling their motion as a solution to the 3-body problem [14]. Previously, quasi-periodic orbits (QPOs) have been computed in this coherent model [14, 15].

The Hill Restricted 4-Body Problem (HR4BP), developed by Scheeres [16] in 1998, is another coherent time periodic model describing the motion of a small body (P_3) in the presence of three large bodies (P_0 , P_1 , and P_2). The model is a higher fidelity model than the CR3BP and BCP, more accurately represents the true dynamics in the Sun-Earth-Moon (SEM) system, is easier to implement than the QBCP, and has previously been used to study the Sun’s effect on the EM system [16–18]. Specifically, periodic orbits and quasi-periodic orbits (QPOs) related to the EM libration points have been computed [18–21], as have connections between Sun-Earth and EM libration point orbits [22]. Olikara, Gómez, and Masdemont [18] computed the HR4BP periodic orbit families corresponding to the CR3BP EM L_1 and L_2 points, the L_1 Lyapunov orbit with $T = \pi$, as well as two additional periodic orbit families existing near a broken pitchfork bifurcation in the dynamical equivalent of the EM L_2 point. Sanaga and Howell [23] computed several orbit families in the HR4BP corresponding to synodic resonant halo orbits. In that work, the authors presented an additional dynamical model, a reduced model of the HR4BP referred to as the RHR4BP [23]. In this work, by using a methodology that leverages a Melnikov-type function and techniques related to detecting bifurcation points, we will present a more detailed picture of the periodic orbits that exist in the HR4BP.

2 Problem Formulation

2.1 Formulation of the HR4BP

The equations of motion for the HR4BP were originally presented by Scheeres [16]. Let P_0 represent the largest body, P_1 and P_2 represent the two other bodies with non-negligible mass, and P_3 be a body with negligible mass near P_1 and P_2 . $\mathcal{B} : \{ \hat{i}_m, \hat{j}_m, \hat{k} \}$ is defined as a rotating frame with a constant angular velocity (with respect to inertial space) in the direction $\hat{\Omega} = \hat{k}$ and an origin at the center of mass of P_1 , P_2 , and P_3 . Note P_0 , P_1 , and P_2 lie in the xy -plane (i.e., the plane perpendicular to \hat{k}). All vector components in this work are presented in the \mathcal{B} -frame. Visual representations of this frame, an intermediate frame used in [16], and terms defined later in this section are provided in Figure 1, where the magenta circle is the total system center of mass and the purple circle is the center of mass of P_1 , P_2 , and P_3 .

Let M_i represent the mass of body P_i . P_1 and P_2 are referred to as the primaries. n_0 represents the mean motion of P_0 considering a 2-body system of P_0 as one body and treating the two primaries as one combined body at \mathbf{R}_c . μ represents the mass ratio of P_1 and P_2 , and m represents the relationship between the period of \mathbf{R}_c about the total system center of mass and the period of P_1 and P_2 about \mathbf{R}_c [18]. n represents the mean motion of the primaries in the 2-body system of P_1 and P_2 . We will assume $\mathbf{R}_c \approx \mathbf{a} = d_a \hat{i}$ where d_a is the distance between the Sun and the Earth-Moon barycenter [16].

Let $[\Phi(\tau, \tau_0)] = \frac{\partial \mathbf{X}}{\partial \mathbf{X}_0}$ be the state transition matrix, $[\Psi(\tau, \tau_0)] = [\Psi_m \ \Psi_\mu] = \left[\frac{\partial \mathbf{X}}{\partial m} \ \frac{\partial \mathbf{X}}{\partial \mu} \right]$, $[A] = \frac{\partial \mathbf{X}'}{\partial \mathbf{X}}$ be the Jacobian matrix, and $[C] = \left[\frac{\partial \mathbf{X}'}{\partial m} \ \frac{\partial \mathbf{X}'}{\partial \mu} \right]$. Note \mathbf{X}_0 refers to the state at initial time τ_0 , $[\Phi(\tau_0, \tau_0)] = [I_{6 \times 6}]$, and $[\Psi(\tau_0, \tau_0)] = [0_{6 \times 2}]$. Under the assumption $\boldsymbol{\Omega} = \hat{\mathbf{k}}$, the equations to integrate \mathbf{X} , $[\Phi]$, and $[\Psi]$ are:

$$(5a) \quad \mathbf{X}' = \begin{bmatrix} \mathbf{r}' \\ -2(1+m)\boldsymbol{\Omega} \times \mathbf{r}' + \nabla V \end{bmatrix}$$

$$(5b) \quad [\Phi]' = [A][\Phi]$$

$$(5c) \quad [\Psi]' = [A][\Psi] + [C]$$

It is important to note that when $m \rightarrow 0$, the HR4BP equations of motion take on the form of the CR3BP equations of motion. As m increases from zero, the effect of the more massive body on the system becomes more pronounced, and $m_{\text{SEM}} = 0.0808$ for the SEM system. In addition to being a periodically forced system, there are also important symmetries in the equations of motion [16, 23].

$$(6a) \quad S_1 : (x, y, z, x', y', z', k\pi + \tau) \rightarrow (x, -y, z, -x', y', -z', k\pi - \tau)$$

$$(6b) \quad S_2 : \left(x, y, z, x', y', z', k\pi + \frac{\pi}{2} + \tau\right) \rightarrow \left(x, -y, z, -x', y', -z', k\pi + \frac{\pi}{2} - \tau\right)$$

As an example, from [16], if the initial condition $\mathbf{X}(\tau = \tau_0) = [x_0, y_0, 0, x'_0, y'_0, 0]^T$ corresponds to a periodic orbit with a period that is an integer multiple of π , then $\mathbf{X}(\tau = -\tau_0) = [x_0, -y_0, 0, -x'_0, y'_0, 0]^T$ also corresponds to a periodic orbit with the same period. This symmetry will be an important consideration when computing periodic orbits.

2.2 Melnikov Theory

When a time-periodic perturbation is added to an autonomous system, a single structure in the autonomous system may have multiple “dynamical equivalents” in the perturbed system (i.e., related structures that exist in the perturbed system). For example, at least four dynamical equivalents to the 9:2 NRHO in the BCP have been identified previously [11]. In that system the continuation of these orbits followed many possible paths, and we expect a similarly complicated behavior in the HR4BP. Melnikov theory is one of the tools we can use to analyze these perturbed systems. For an introduction to classical Melnikov theory, which was originally presented by Melnikov [24], we refer the reader to sections 3.1 and 3.2 of [25], but additional detail can be found in Chapter 28.1 of [26], Chapter 4.5 of [27], and Chapter 4.9 of [28].

This theory has been improved, extended, and applied to a variety of different systems, including those with higher dimensions [26, 29–33]. By considering an expansion of the “energy principle” (the change in energy at the start and end of any periodic orbit must be zero), Cenedese and Haller [34] present an expression for a Melnikov-type function that is applicable to our study of orbits in the HR4BP. It is this Melnikov-type function of [34] that we will use in our analysis, which we will simply refer to as the Melnikov function. We will now present the basic form of the Melnikov function from [34]. Say the acceleration of an autonomous system (in our case the CR3BP) is given by $\ddot{\mathbf{r}} = \mathbf{f}(\mathbf{X})$. Let the flow of the vector field in this autonomous system be defined as $\mathbf{X}(\tau) = \varphi(\mathbf{X}_0, \tau)$. Say a small perturbation is added so that the new acceleration is

$$(7) \quad \ddot{\mathbf{r}} = \mathbf{F} = \mathbf{f}(\mathbf{X}) + \varepsilon \mathbf{g}(\mathbf{X}, \tau_0 + \tau; T_g, \varepsilon)$$

where \mathbf{g} is time-periodic with period T_g so $\mathbf{g}(\mathbf{X}, \tau_0 + \tau; T_g, \varepsilon) = \mathbf{g}(\mathbf{X}, \tau_0 + \tau + T_g; T_g, \varepsilon)$, ε is the perturbation parameter, and τ corresponds to time relative to τ_0 .

Periodic orbits in this system must have a minimal period (T) that is in some resonance with the forcing period (T_g) where $T_g = \pi$ for the HR4BP (i.e., $T = bT_g$ where b is a positive integer) [35]. Say there is a specific periodic orbit \mathcal{Z} in the unperturbed autonomous system of

period T^* which satisfies the appropriate resonance condition with T_g (i.e., $bT_g = aT^*$ where a and b are relatively prime integers), and an initial state time history of the orbit in the unperturbed system is generated using a specific state ${}^*\mathbf{X}_s$ on the orbit. As the periodic orbit exists in the autonomous system, any point on that orbit ${}^*\mathbf{X}(s) = \varphi({}^*\mathbf{X}_s, s)$ where $s \in [0, T^*)$ could be used as the initial state to generate the same periodic orbit, but with a different time history associated with each state. So, based on the particular value of s , the periodic orbit state time history in the unperturbed system can be represented as ${}^*\mathbf{X}(s + \tau) = \varphi({}^*\mathbf{X}_s, s + \tau)$ for $\tau \in [0, T^*]$ where ${}^*\mathbf{X}(s + \tau) = {}^*\mathbf{X}(s + \tau + T^*)$ and $s \in [0, T^*)$. With that in mind, the value of the Melnikov function takes the form:

$$(8) \quad \mathcal{M}(s, \tau_0) = \int_0^{aT^*} \mathbf{g}({}^*\mathbf{X}(s + \tau), \tau_0 + \tau) \cdot {}^*\mathbf{r}'(s + \tau) d\tau$$

which is dependent on the choice of the initial point on the unperturbed periodic orbit (i.e., the value of s) and the initial time τ_0 . Note that we have removed the T_g and ε terms from this equation for conciseness, and the period of the orbit in the perturbed system corresponding to the orbit in the unperturbed system is $T = bT_g$.

For an orbit to be a periodic solution, there must be no work done by the perturbation force on the orbit over one period. The zeros of the Melnikov function represent where this is the case (at least when considering the leading order terms). Provided $\mathcal{M}(s, \tau_0)$ is not identically zero for all $s \in [0, T^*)$, we expect to be able to continue periodic orbits from the unperturbed system into the perturbed system at the points s on the unperturbed orbit provided the initial time when beginning the integration is τ_0 . Points where this function is zero are points where we will attempt to continue CR3BP orbits into the HR4BP.

3 Methodology

As this system is non-autonomous, we do not expect to identify families of periodic orbits as we would in an autonomous system [36]. However, we do expect to identify periodic orbit “families” in the HR4BP if we fix the value of T and initial time (τ_0), and perform a continuation while allowing the initial state ($\mathbf{X}_0 = \mathbf{X}(\tau = \tau_0)$) and at least one of the parameters m and/or μ to vary. The phrase “HR4BP periodic orbit family” will refer to the “family” that can be computed starting from a specific periodic orbit in the HR4BP and then allowing \mathbf{X}_0 and m to vary. To compute these families we will first expand the HR4BP equations of motion about $m = 0$. We will then use this expansion when evaluating the Melnikov function for orbits in the EM CR3BP with appropriate periods. We will use pseudo-arclength continuation starting at $m = 0$ to compute the corresponding HR4BP periodic orbit families. We will start at the five libration points whose HR4BP orbits have periods of $T = \pi$, and at each state on the selected CR3BP periodic orbits where $\mathcal{M}(s, \tau_0) = 0$. We will then identify bifurcations along these families in order to compute additional families starting at non-zero values of m . Note we will always use $\tau_0 = 0$ unless explicitly stated otherwise.

3.1 Expanding the HR4BP Equations of Motion

In order to use the Melnikov function presented in (8), we need to expand the HR4BP equations of motion in (5) about $m = 0$ so they are in the form of (7). This expansion will result in $\varepsilon \mathbf{g} = \mathbf{g}_1 m + \mathbf{g}_2 m^2 + \mathbf{g}_3 m^3 + \dots$. By using $\varepsilon = m$, the leading order term can be used as \mathbf{g} in (8) (i.e., $\mathbf{g} = \mathbf{g}_1$). While the definition of M given in (16b) will be used for all calculations except when evaluating the Melnikov function. In this case, the definition $M = m$ will be used which results in different values for the Hill variation orbit coefficients: $d_0 = 1$, $d_1 = -2/3$, $d_2 = 7/18$, $d_3 = -4/81$, $c_{-1,2} = -19/16$, $c_{1,2} = 3/16$, $c_{-1,3} = -5/3$, and $c_{1,3} = 1/2$. Note that these are the same values that are presented in [16]. Let $\mathbf{R}_{1-\mu,C}$ and $\mathbf{R}_{\mu,C}$ be the relative position of P_3 with respect to P_1 and P_2 , respectively, in the CR3BP (i.e., when $m = 0$). Performing this expansion we obtain the

following result for \mathbf{g}_1 :

$$(9a) \quad \mathbf{g}_1 = 2 \begin{bmatrix} y' \\ -x' \\ 0 \end{bmatrix} + 2 \begin{bmatrix} x \\ y \\ 0 \end{bmatrix} + 3d_1 \left(\frac{1-\mu}{R_{1-\mu,C}^3} \mathbf{R}_{1-\mu,C} + \frac{\mu}{R_{\mu,C}^3} \mathbf{R}_{\mu,C} \right)$$

$$(9b) \quad \mathbf{g}_1 = 2\boldsymbol{\Omega} \times \mathbf{r}' + 2\mathbf{f}$$

$$(9c) \quad \mathbf{g}_2 = 3\boldsymbol{\Omega} \times \mathbf{r}' + \frac{3}{2}\mathbf{f} + \mathbf{h}_2$$

$$(9d) \quad \mathbf{g}_3 = \mathbf{h}_3$$

Note $(\boldsymbol{\Omega} \times \mathbf{r}') \cdot \mathbf{r}' = 0$ and \mathbf{f} corresponds to the acceleration in the CR3BP, so integrating $\mathbf{g}_1(*\mathbf{X}(s+\tau), \tau_0+\tau) \cdot *\mathbf{r}'(s+\tau)$ (i.e., computing the Melnikov function) will always result in a value of zero. The underlying culprit responsible for this result is the way time is scaled in the HR4BP, which is based on the value of m according to the relationship defined in (2c). To first order, the primary effect from the perturbation capturing the effect of P_0 is associated with the scaling of time introduced in the formulation of the HR4BP. From the previous discussion related to $(\boldsymbol{\Omega} \times \mathbf{r}') \cdot \mathbf{r}' = 0$ and \mathbf{f} , only the \mathbf{h}_k terms in (9) have the potential to do any work. Let $\alpha = \tau_0 + \tau$ for conciseness. Expressions for \mathbf{h}_2 and \mathbf{h}_3 are provided in (10).

$$(10a) \quad \mathbf{h}_2(\mathbf{X}, \alpha) = -\frac{3}{2} \begin{bmatrix} -\cos(2\alpha) & \sin(2\alpha) & 0 \\ \sin(2\alpha) & \cos(2\alpha) & 0 \\ 0 & 0 & 2/3 \end{bmatrix} \mathbf{r} - \frac{1}{8}(1-\mu)\mu[P] \begin{bmatrix} -8\cos(2\alpha) \\ 11\sin(2\alpha) \\ 0 \end{bmatrix}$$

$$(10b) \quad \mathbf{h}_3(\mathbf{X}, \alpha) = -\frac{1}{12}(1-\mu)\mu[P] \begin{bmatrix} -38\cos(2\alpha) \\ 59\sin(2\alpha) \\ 0 \end{bmatrix}$$

$$(10c) \quad [P] = \left(\frac{1-\mu}{R_{1-\mu,C}^3} - \frac{\mu}{R_{\mu,C}^3} \right) [I_{3 \times 3}] - \frac{3}{R_{1-\mu,C}^5} \mathbf{R}_{1-\mu,C} \mathbf{R}_{1-\mu,C}^T + \frac{3}{R_{\mu,C}^5} \mathbf{R}_{\mu,C} \mathbf{R}_{\mu,C}^T$$

As we can ignore the contribution from \mathbf{g}_1 , the perturbation $\varepsilon\mathbf{g}$ takes the form $m^2\mathbf{g}_2 + m^3\mathbf{g}_3 + \dots$. So, by using $\varepsilon = m^2$ and ignoring higher order terms, the Melnikov function takes the form of:

$$(11) \quad \mathcal{M}(s, \tau_0) = \int_0^{aT^*} \mathbf{h}_2(*\mathbf{X}(s+\tau), \tau_0+\tau) \cdot *\mathbf{r}'(s+\tau) d\tau$$

If the Melnikov function in (11) is identically zero for any $s \in [0, aT^*]$ on a specific CR3BP periodic orbit, then we will use the next order of \mathbf{h}_j instead of \mathbf{h}_2 in (11). Note that the validity of using a higher order \mathbf{h}_j is contingent upon using $\varepsilon = m^j$ and the assumptions related to the behavior of the orbit presented in Appendix B.1 being valid with this new ε .

3.2 Behavior of the HR4BP Melnikov Function

To determine points on a CR3BP periodic orbit we expect to be able to continue into the HR4BP for $m > 0$, zeros of the Melnikov function need to be identified. This could be accomplished by selecting a value of τ_0 , discretizing the CR3BP periodic orbit into a set of different points (i.e., selecting different values of s), and then integrating (11) to determine the Melnikov function at each point. However, we have developed three propositions related to the behavior of the Melnikov function that demonstrate this procedure is unnecessary. Please refer to Appendix B for the relevant proofs. Proposition 1 is generally valid for the generic form of the Melnikov function presented in (8). The other two, Proposition 2 and Proposition 3, were derived for the specific form of (11) using the definition of \mathbf{h}_2 in (10a). However, it should be noted that these two propositions are also valid for the specific form of (11) if the definition of \mathbf{h}_3 in (10b) is used instead of \mathbf{h}_2 . Furthermore, we expect that there are similar propositions that will be valid for other of systems similar to the HR4BP, such as the ER3BP, the BCP, and the QBCP.

Proposition 1. Assume $\mathcal{M}(s, \tau_0)$ is a Melnikov function of the form shown in (8), where s is an initial point on the unperturbed periodic orbit, and τ_0 is the initial time corresponding to the periodic perturbation. Let $T = bT_g$ be the period of the periodic orbit in the perturbed system, where $b \in \mathbb{Z}_+$ and T_g is the period of the forcing. Then, the following results hold for any $\tau_s \in \mathbb{R}/T\mathbb{Z}$:

- (a) $\mathcal{M}(s + \tau_s, \tau_0 + \tau_s) = \mathcal{M}(s, \tau_0)$
- (b) $\mathcal{M}(s + \tau_s, \tau_0) = \mathcal{M}(s, \tau_0 - \tau_s)$

Proposition 1(a) is a somewhat intuitive result. The Melnikov function does not change if an equal shift is applied to the initial point on the unperturbed orbit and the the initial value of time used in the integration. Proposition 1(b) indicates that shifting the point along the initial unperturbed orbit produces the same Melnikov function as shifting the initial time of integration by an equal amount in the opposite direction. This result is known to apply to the original form of the Melnikov function as shown in [37], so it is not surprising it applies to this Melnikov-like function as well.

Proposition 2. Assume $\mathcal{M}(s, \tau_0)$ is the Melnikov function defined in (11) using either \mathbf{h}_2 in (10a) or \mathbf{h}_3 in (10b), s is an initial point on the unperturbed periodic orbit, and τ_0 is the initial time corresponding to the periodic perturbation. Let $T = bT_g$ be the period of the periodic orbit in the perturbed system, where $b \in \mathbb{Z}_+$ and T_g is the period of the forcing. Then, the following relations hold for any $\tau_s \in \mathbb{R}/T\mathbb{Z}$:

- (a) $\mathcal{M}(s, \tau_0 + \tau_s) = \cos(2\tau_s)\mathcal{M}(s, \tau_0) - \sin(2\tau_s)\mathcal{M}(s, \tau_0 - \frac{\pi}{4})$
- (b) $\mathcal{M}(s + \tau_s, \tau_0) = \cos(2\tau_s)\mathcal{M}(s, \tau_0) + \sin(2\tau_s)\mathcal{M}(s + \frac{\pi}{4}, \tau_0)$

Proposition 2 has two forms: Proposition 2(a) and Proposition 2(b). By Proposition 2(b), the Melnikov function at any point can be determined from knowledge of the Melnikov function at two initial points on the unperturbed orbit, i.e., (11) must be integrated only twice to determine $\mathcal{M}(s, \tau_0)$ and $\mathcal{M}(s + \frac{\pi}{4}, \tau_0)$. By specifying a set of different τ_s values in the range $[0, aT^*)$, Proposition 2(b) can then be used to directly obtain $\mathcal{M}(s, \tau_0)$ at any other value of $s = s + \tau_s$. Proposition 1(b) can then be used to obtain $\mathcal{M}(s, \tau_0)$ at any other value of τ_0 .

There are a couple other important implications of Proposition 2. First, for a particular value of s and τ_0 , if $\mathcal{M}(s, \tau_0) = 0$ then $\mathcal{M}(s + k\frac{\pi}{2}, \tau_0) = 0$ for $k \in \mathbb{Z}$. Second, for a particular value of s and τ_0 , if $\mathcal{M}(s, \tau_0) = 0$ and $\mathcal{M}(s + \frac{\pi}{4}, \tau_0) = 0$ then the Melnikov function is identically zero for any other value of s and τ_0 on that particular periodic orbit. If this is the case, then as discussed previously, we attempt to evaluate the Melnikov function using a higher order \mathbf{h}_j , provided the necessary assumptions are still valid for $\varepsilon = m^j$.

Proposition 3. Assume $\mathcal{M}(s, \tau_0)$ is the Melnikov function defined in (11) using either \mathbf{h}_2 in (10a) or \mathbf{h}_3 in (10b). When evaluated at an initial point on a CR3BP periodic orbit with a period T^* that satisfies the half-period symmetry conditions in (13), the Melnikov function takes the following simplified form:

$$(12a) \quad \mathcal{M}(s, \tau_0) = 2AB$$

$$(12b) \quad A = \begin{cases} \sin(2\tau_0), & \text{if } a = 1 \\ 0, & \text{otherwise} \end{cases}$$

$$(12c) \quad B = \int_0^{T^*/2} (K(*\mathbf{X}(s + \tau)) \cos(2\tau) - J(*\mathbf{X}(s + \tau)) \sin(2\tau)) d\tau$$

Expressions for the terms J and K in (12c) are provided in Appendix B in (35) and (44). Note all five of the conditions in (13) must be met for all values of $\tau \in [0, T^*/2]$ for the statement of half-period symmetry to be true. Some examples of such points are states on the CR3BP L_1 and L_2 planar Lyapunov and halo orbits that lie on the xz -plane.

$$(13a) \quad {}^*x(s + T^* - \tau) = {}^*x(s + \tau)$$

$$(13b) \quad {}^*x'(s + T^* - \tau) = -{}^*x'(s + \tau)$$

$$(13c) \quad {}^*y(s + T^* - \tau) = -{}^*y(s + \tau)$$

$$(13d) \quad {}^*y'(s + T^* - \tau) = {}^*y'(s + \tau)$$

$$(13e) \quad {}^*z(s + T^* - \tau) {}^*z'(s + T^* - \tau) = - {}^*z(s + \tau) {}^*z'(s + \tau)$$

For the Melnikov function in (12a) to be zero, A and/or B must be zero. Based on the form of A and B , identifying when $A = 0$ is trivial. By inspection, if a CR3BP periodic orbit has a period $T^* = k\pi$, $k \in \mathbb{Z}^+$ (i.e., if $a = 1$), then any points on that orbit that satisfy the half-period symmetry conditions presented in (13) are points where $A = 0$ provided $\tau_0 = k_1 \frac{\pi}{2}$, $k_1 \in \mathbb{Z}$ based on (12b). For example, let us consider the CR3BP L_1 and L_2 planar Lyapunov and halo periodic orbits with $T^* = \pi$. All points on these orbits that lie on the xz -plane are points where we expect to be able to continue a corresponding HR4BP periodic orbit family with $\tau_0 = 0$. If T^* is not an integer multiple of π (i.e., if $a > 1$), but there is at least one point on the orbit that satisfies (13), then the Melnikov function is identically zero when using \mathbf{h}_2 . As using \mathbf{h}_3 instead of \mathbf{h}_2 will produce the same results, the Melnikov function should be recomputed with \mathbf{h}_4 .

3.3 Generating HR4BP Periodic Orbit Families

The initial set of generated orbit families in the HR4BP were the five EM libration points and periodic orbits in the CR3BP whose periods were an integer multiple of π . Please note that for the remainder of this work, when a libration point is referenced, it will refer to an EM libration point. These orbit families were continued until either the maximum m value at which the orbit of the primaries is stable was reached ($m = 0.19510486$) [16], or the continuation algorithm failed to identify a new orbit member. Other families were computed by identifying bifurcation points in this set of initial families. To identify potential bifurcation points, a singular value decomposition (SVD) on a modified form of the corrections Jacobian was performed. The modified form of the corrections Jacobian ($[DB]$) is presented in (14).

$$(14) \quad [DB] = [[\Phi(T, 0)]^{n_B} - [I_{d \times d}], [\Psi_m(n_B T, 0)]]$$

where $[\Phi(T, 0)]$ is the monodromy matrix of the periodic orbit, and $[\Psi_m(\tau, 0)] = \left. \frac{\partial \mathbf{X}}{\partial m} \right|_{\tau}$. For tangent bifurcations, period-doubling bifurcations, or other period-multiplying bifurcations ($n_B T$ bifurcations where n_B is an integer) in the original family, n_B should be set to 1, 2, or n_B respectively. Note new families were only computed at tangent bifurcation points in this study.

As $[DB]$ is a 6×7 matrix, one of its singular values will be 0. Let σ_α and σ_β represent the smallest and second smallest non-zero singular values, respectively. Points on the HR4BP orbit families where a local minimum in either σ_α or σ_β were identified were potential bifurcation points. To compute a different orbit family at these points, the vector ($\delta \mathbf{V}_\sigma$) corresponding to either σ_α or σ_β (depending on which reached a local minimum) was used along with the initial state and m value on the original family (\mathbf{X}_0^A and m^A , respectively). The initial guess for an orbit on the new family is then represented as:

$$(15) \quad V_0^B = \begin{bmatrix} \mathbf{X}_0^A \\ m^A \end{bmatrix} + \Delta s_0 \delta \mathbf{V}_\sigma$$

It is important to note that if the components in $\delta \mathbf{V}_\sigma$ corresponding to the initial state are aligned in some manner with the symmetries in (6), then it is possible that multiple new orbit families may exist near that bifurcation point. For example, if the initial state at $\tau = 0$ is $\mathbf{X}_0^A = [x_0, 0, 0, 0, y_0', 0]^T$ and the components of $\delta \mathbf{V}_\sigma$ corresponding to the initial state are $[0, \delta y_0, 0, \delta x_0', 0, 0]^T$, then both the $+$ and $-$ directions should be used to potentially generate multiple new families. The new families were continued using the same pseudo-arclength continuation scheme used for the original families. The members of those periodic orbit families where $m = m_{\text{SEM}}$ are the periodic orbits in the HR4BP SEM system. It should be noted that if a family has a clear symmetry, then additional orbits may be obtained by applying the appropriate transformation (e.g., to obtain the southern butterfly orbit equivalent to the northern butterfly orbit).

4 Periodic Orbits

The value of the Melnikov function evaluated with $\tau_0 = 0$ at different points on the CR3BP L_4 planar orbit member with $T^* = 2\pi$ (so $a = 1$ and $b = 2$) is shown in Figure 2. The four zeros of the Melnikov function are the starting points for four HR4BP orbit families which are also shown in Figure 2. It is important to note that these four HR4BP orbit families have been identified and computed previously by Scheeres [16] and Peterson et al. [21] using other techniques. However, the techniques we use leveraging the Melnikov function are more general. To validate our techniques, 100 points were selected on the initial CR3BP L_4 planar 2π periodic orbit, and the continuation procedure was attempted starting at each of these points. Four of these points produced families in the HR4BP that could be continued up to to values of m that were not negligible. These four points matched the four points where the Melnikov function is zero.

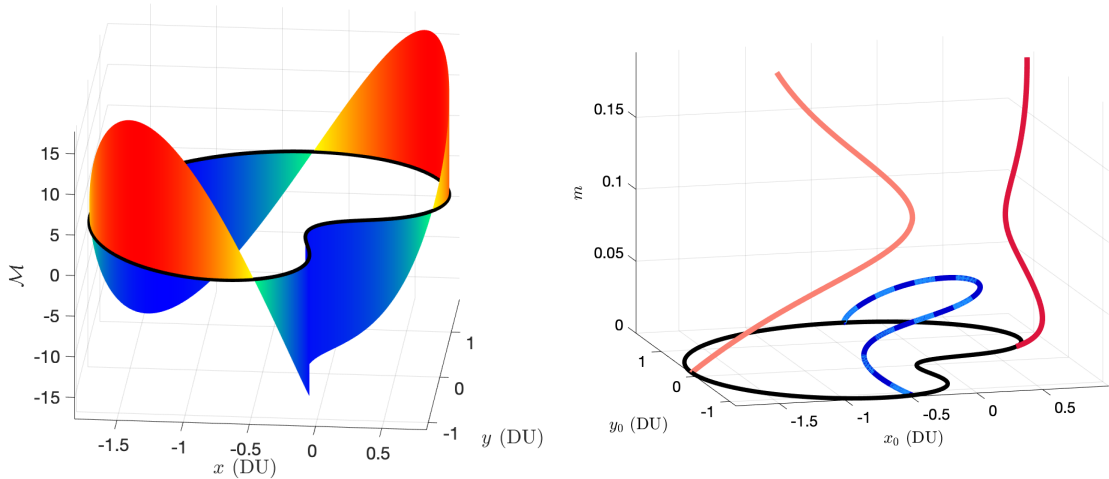


Fig. 2: Continuing the CR3BP L_4 Planar Orbit with $T^* = 2\pi$ into the HR4BP. Left: Melnikov function $\mathcal{M}(s, 0)$ values. Right: HR4BP periodic orbit families hodograph.

Determining the number of distinct orbit families that can be generated in the HR4BP from a single orbit in the CR3BP is of interest. For the discussion related to this topic, we will distinguish between an “orbit”/“orbit family” and an “object”/“object family”. An “orbit” refers to the collection of states on an orbit with the specific values of τ at those states. An “object” refers to the collection of states on an orbit irrespective of τ at those states. Using this terminology, a single object can contain the states corresponding to multiple different orbits. For example, two points on the CR3BP L_2 Northern Halo family member with $T = \pi$ can be continued (using Proposition 3) to produce two different HR4BP orbit families. At a particular value of m , the orbits in these two families contain the same states, with their corresponding values of τ shifted by $\pi/2$. Therefore, only one object family in the HR4BP was identified corresponding to that particular CR3BP orbit. Note that the continuation of the orbits shown in Figure 3 starts with m increasing (from yellow to magenta), before decreasing (from magenta to dark blue), until the CR3BP L_2 Southern Halo orbit with $T = \pi$ is obtained.

The L_1 vertical orbit with $T^* = \pi$ ($a = 1$ and $b = 1$) has four points that satisfy the symmetry conditions in (13). These points are separated from each other by $\tau_s = \pi/4$, so by Proposition 3 and Proposition 2(b) the Melnikov function is identically zero for this orbit. We reevaluated the Melnikov function using \mathbf{h}_4 and found four zeros corresponding to the four points on the xz -plane. Each of these points produced a different HR4BP orbit family which belonged to one of three different object families which are shown in Figure 4. Note that the object family on the right side of Figure 4 consists of two different orbit families. The different colors are simply to distinguish between members along each family.

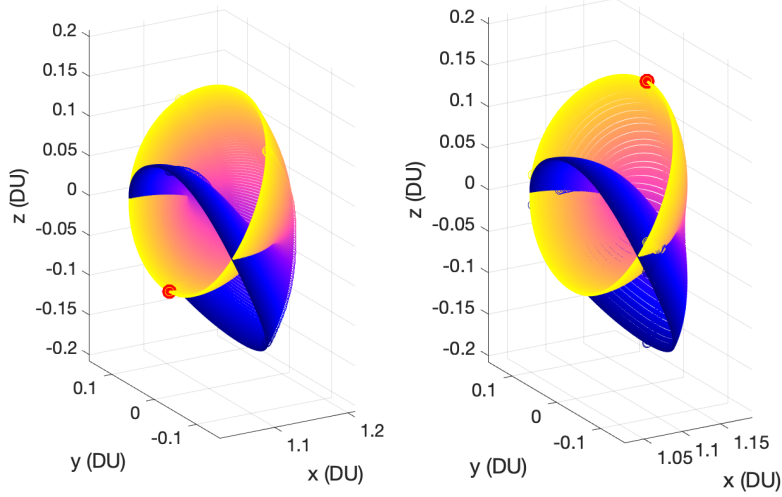


Fig. 3: HR4BP Periodic Orbit Families Corresponding to the CR3BP L_2 N/S Halo Orbit with $T = \pi$.

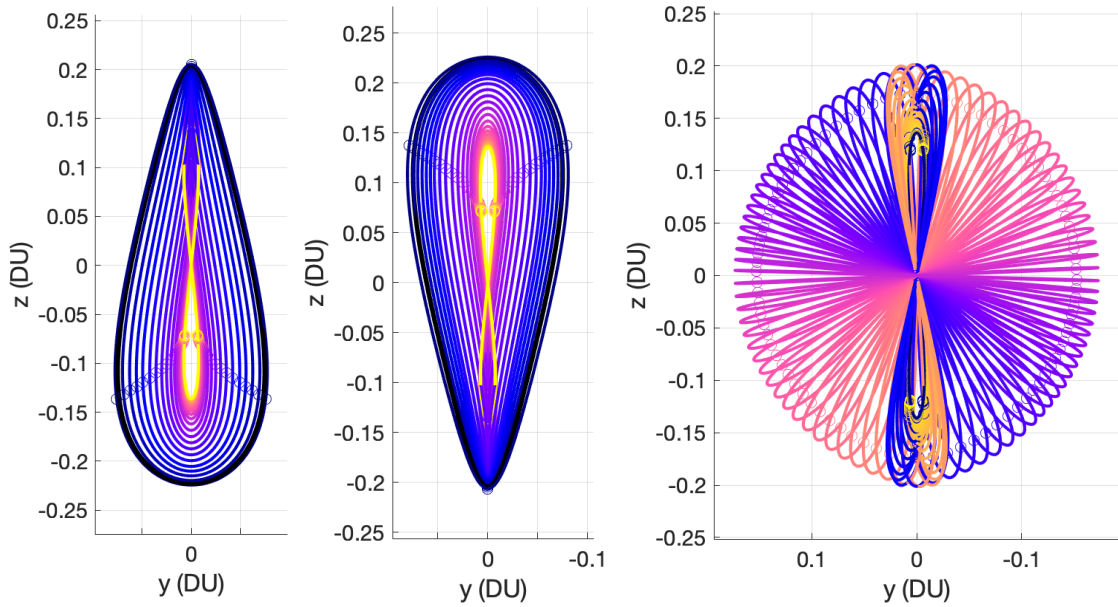


Fig. 4: HR4BP Periodic Orbit Families Corresponding to the CR3BP L_1 Vertical Orbit with $T^* = \pi$.

4.1 Families from EM Libration Points and Associated Periodic Orbits

Diagrams depicting the orbit families identified around L_2 are presented in Figure 5 where each color represents a different family. The gray plane represents the value of m for the SEM system. The position components in these plots correspond to the initial states at $\tau_0 = 0$. The initial set of orbits used that were related to L_2 were the CR3BP L_2 point ($T = \pi$, shown in maroon) or the A family, the planar Lyapunov family member with $T = 2\pi$ (shown in dark red and dark orange), the vertical family member with $T = 2\pi$ (shown in orange), the northern (and southern) halo family member with $T = \pi$ (shown in gold and light green), the northern (and southern) butterfly family member with $T = \pi$ (shown in green and aquamarine), and the 9:2 near-rectilinear halo orbit (NRHO) with $T = 4\pi$ (shown in teal and light blue). Families identified from bifurcations in the initial families are indicated by magenta through cyan lines. Bifurcation diagrams showing the normalized values of σ_α and σ_β along the families are provided in Figure 6. Purple represents the family maximum and yellow represents zero.

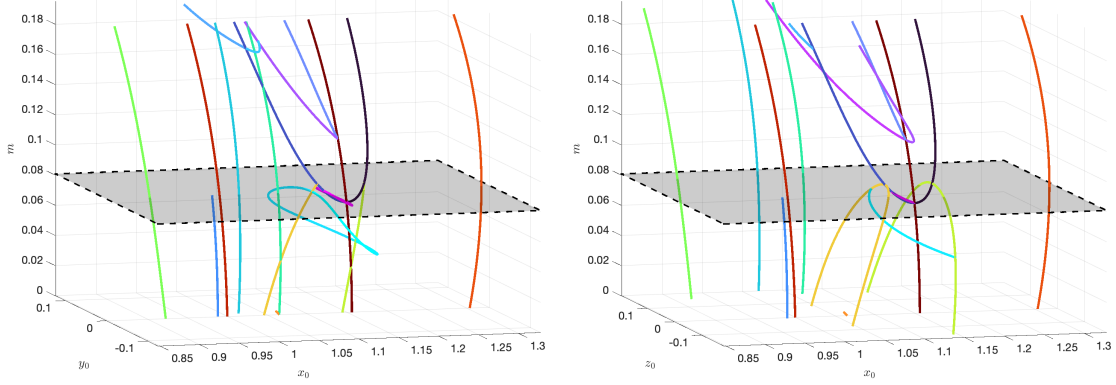


Fig. 5: Hodographs of HR4BP Periodic Orbit Families Near L_2 with initial states at $\tau_0 = 0$.

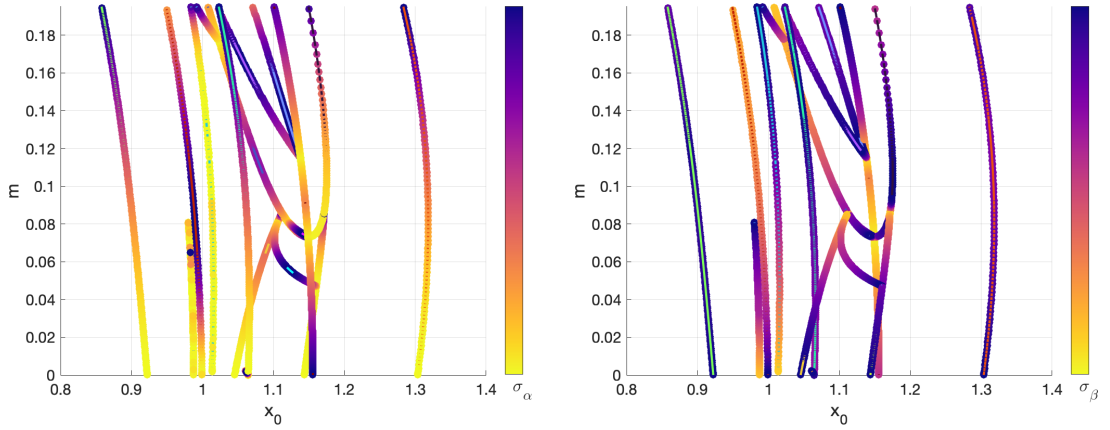


Fig. 6: σ_α (left) and σ_β (right) with $n_B = 1$ for the EM L_2 HR4BP Periodic Orbits.

Locations in Figure 6 where local minima are reached indicate potential bifurcation points. As can be seen in these plots, many points corresponding to these local minima are where multiple families intersect. Note that all three families associated with L_2 identified in [18] (the A, B, and C families) were identified in this work. Note we use a different representation of the Hill variation orbit in this work than the one used in [18]. We expect this representation is the reason for the minute differences between the family structures around bifurcation points in this work and the results in [18].

Diagrams depicting the orbit families identified around L_1 are presented in Figure 7. Bifurcation diagrams showing the normalized values of σ_α and σ_β along the families are provided in Figure 8.

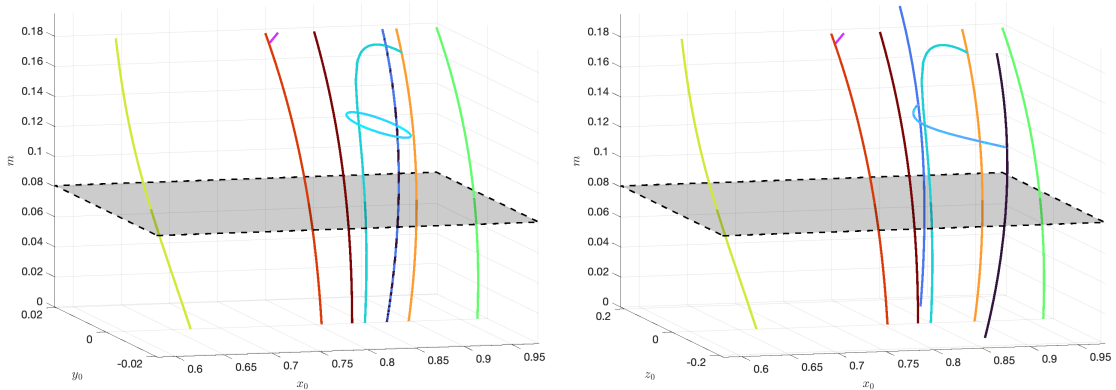


Fig. 7: Hodographs of HR4BP Periodic Orbit Families Near L_1 with initial states at $\tau_0 = 0$.

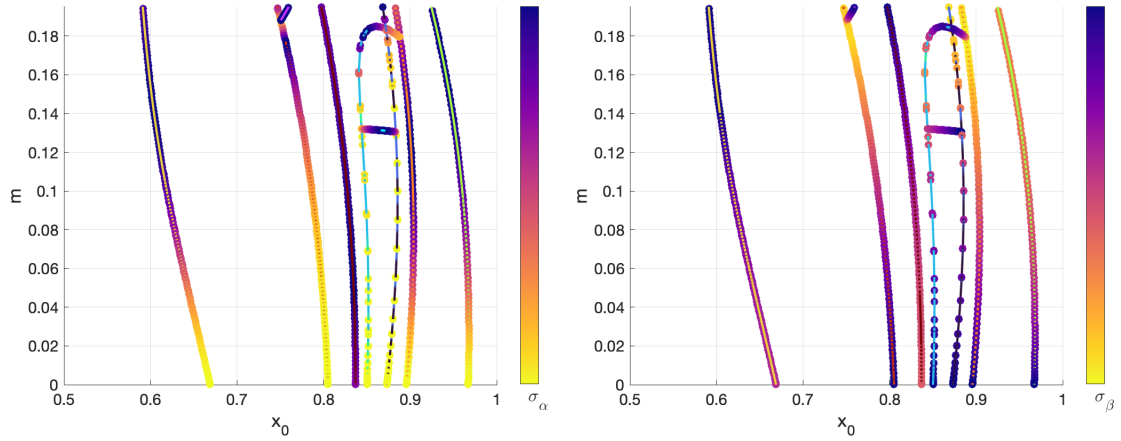


Fig. 8: σ_α (left) and σ_β (right) with $n_B = 1$ for the EM L_1 HR4BP Periodic Orbits.

The initial set of orbits related to L_1 were the CR3BP L_1 point (with $T = \pi$, shown in maroon in Figure 7), the planar Lyapunov family member with $T = \pi$ (shown in red and orange) and $T = 2\pi$ (shown in gold and green), and the vertical family member with $T = \pi$ (shown in aquamarine, light blue, and blue). Families identified from bifurcations in the initial families are indicated by the magenta through cyan lines.

Diagrams depicting the orbit families identified around L_3 , L_4 , and L_5 are presented in Figure 9. Bifurcation diagrams showing the normalized values of σ_α and σ_β along the families are provided in Figure 10.

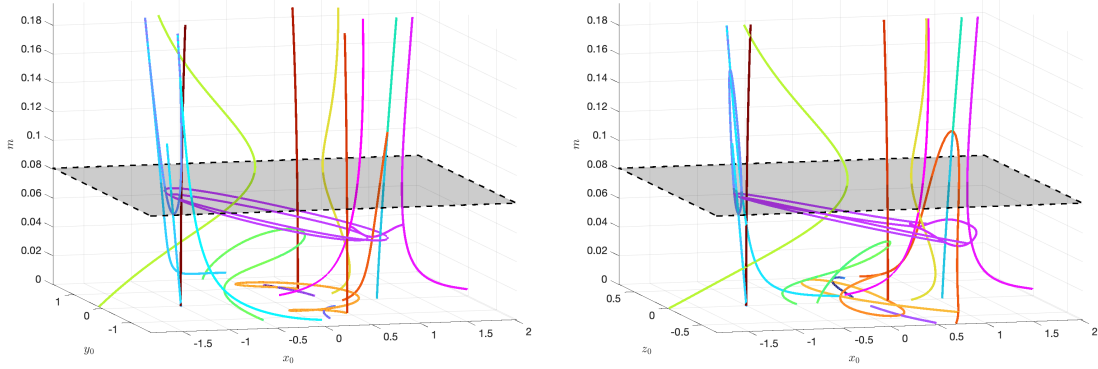


Fig. 9: Hodographs of HR4BP Periodic Orbit Families Near L_3 , L_4 , & L_5 with states at $\tau_0 = 0$.

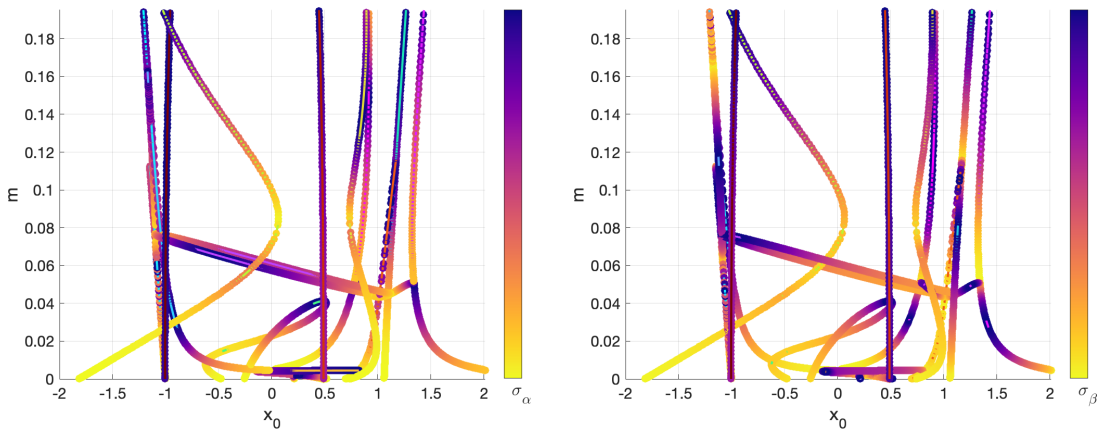


Fig. 10: σ_α (left) and σ_β (right) with $n_B = 1$ for the EM L_3 , L_4 , & L_5 HR4BP Periodic Orbits.

The initial set of orbits related to L_3 , L_4 , and L_5 that were used were those corresponding to the CR3BP L_3 , L_4 , and L_5 points (with $T = \pi$, shown in maroon in Figure 9), the L_4 and L_5 planar Lyapunov family members with $T = \pi$ (shown in red and orange) and $T = 2\pi$ (shown in gold, light green, and green), and the L_3 , L_4 , and L_5 vertical family members with $T = \pi$ (shown in aquamarine, light blue, and blue). Families identified from bifurcations in these initial families are indicated by the magenta through cyan lines.

A collection of the HR4BP periodic orbits that exist in the vicinity of EM libration points at the SEM value of m are depicted in Figure 11. The colors in these plots correspond to the HR4BP families in Figures 5, 7 and 9.

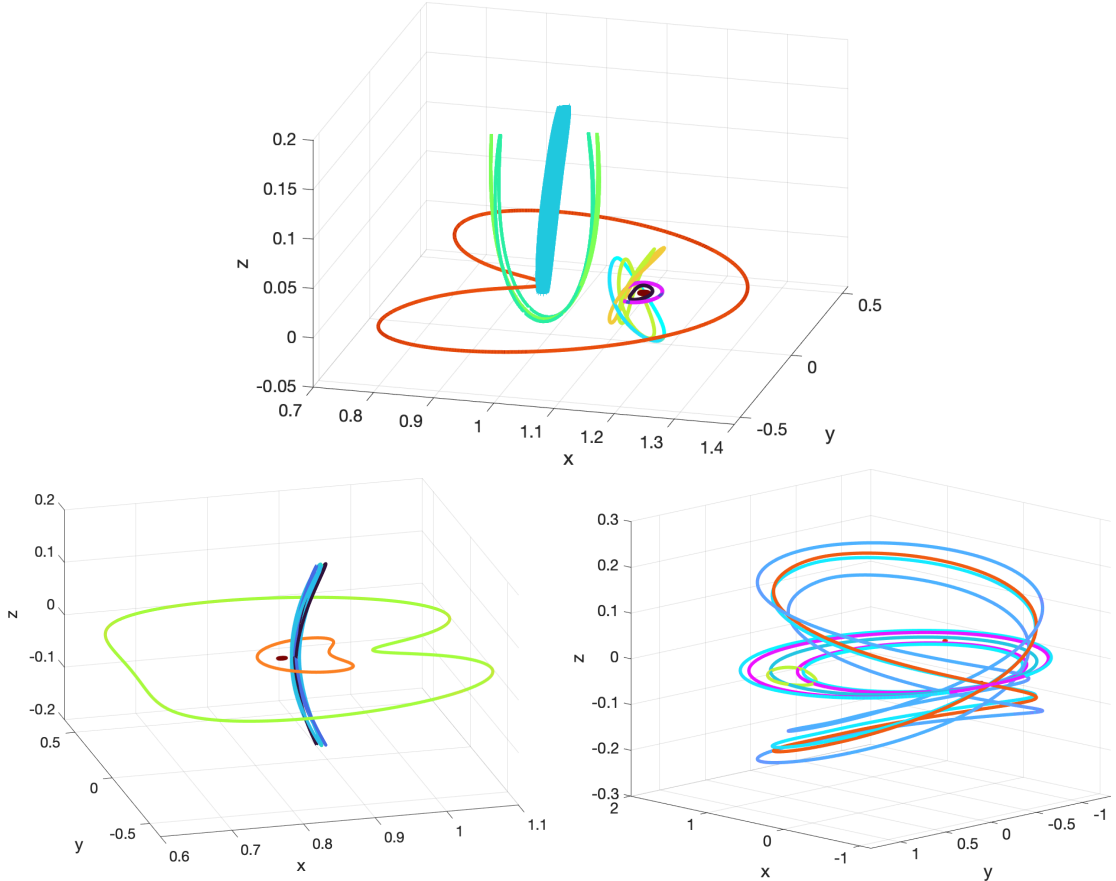


Fig. 11: HR4BP Periodic Orbits Associated with the EM Libration Points in the SEM system.

5 Conclusion

Periodic orbits in the CR3BP (Circular Restricted 3-Body Problem) are useful starting points for obtaining periodic orbits in the HR4BP (Hill Restricted 4-Body Problem). By continuing these orbits up from $m = 0$, many periodic orbit families in the HR4BP can be computed. The set of orbits in these families with $m = 0.0808$ and $\mu = 0.0122$ are periodic orbits in the HR4BP representation of the Sun-Earth-Moon system. By studying the singular values of the corrections Jacobian, leveraging symmetry when applicable, and using other continuation techniques, a variety of periodic orbits can be identified. We expect to find many other families connected to the families identified in this paper by analyzing period-multiplying bifurcations. While additional study is needed to completely map out the periodic orbit structure in the HR4BP, this work presents techniques that can be used to generate resonant periodic orbits in periodically forced systems. We validated these techniques by replicating results of previously computed orbits in the HR4BP, have extended these families to a wider parameter space, and computed additional families originating from periodic orbits around the libration points.

Acknowledgments. This work was carried out with support from U.S. Air Force Office of Scientific Research grant FA9550-21-1-0332.

A HR4BP Equations of Motion

The coefficients for the Hill variation orbit (HVO) are a function of m and are provided in (16) and Tables 1 and 2.

$$(16a) \quad \bar{\rho} = \bar{\xi}\hat{\mathbf{i}}_m + \bar{\eta}\hat{\mathbf{j}}_m + \bar{\zeta}\hat{\mathbf{k}} = \begin{bmatrix} \bar{\xi} \\ \bar{\eta} \\ \bar{\zeta} \end{bmatrix} = \begin{bmatrix} \sum_{n=1}^N (b_n + b_{-n}) \cos 2n\tau \\ \sum_{n=1}^N (b_n - b_{-n}) \sin 2n\tau \\ 0 \end{bmatrix}$$

$$(16b) \quad M = \frac{m}{1 - m/3}$$

$$(16c) \quad a_0 = g_0 \sum_{p=0}^P d_p M^p \quad \text{where} \quad g_0 = M^{2/3}$$

$$(16d) \quad b_n = \frac{a_n}{a_0} = \sum_{p=0}^P c_{n,p} M^p$$

Table 1: Coefficients d_p for the HVO.

p	d_p
0	1
1	-8
2	9
2	133
3	-162
3	-1264
4	2187
4	3319421
5	-5038848
5	-13366211
6	11337408
6	2028830887
7	-244880128
7	-4682845907
8	509880288
8	1922822363821
9	-12694994583552
9	-5982128249099224247
9	3119921868853739520

Table 2: Coefficients $c_{n,p}$ for the HVO.

p	n							
	-4	-3	-2	-1	1	2	3	4
2	0	0	0	$\frac{-19}{16}$	$\frac{3}{16}$	0	0	0
3	0	0	0	$\frac{-7}{8}$	$\frac{3}{8}$	0	0	0
4	0	0	0	$\frac{11}{44}$	$\frac{7}{48}$	$\frac{25}{553}$	0	0
5	0	0	$\frac{23}{640}$	$\frac{5}{36}$	$\frac{-1}{6}$	$\frac{1920}{3743}$	0	0
6	0	$\frac{1}{5237}$	$\frac{3200}{1829}$	$\frac{-361}{374797}$	$\frac{-34589}{110592}$	$\frac{14400}{-22907}$	$\frac{833}{12288}$	0
7	0	$\frac{192}{5237}$	$\frac{3200}{1829}$	$\frac{82944}{374797}$	$\frac{110592}{-22907}$	$\frac{14400}{-28811}$	$\frac{27337}{27337}$	0
8	$\frac{23}{6144}$	$\frac{215040}{263713}$	$\frac{288000}{124719}$	$\frac{276480}{98804551}$	$\frac{46080}{-23804639}$	$\frac{-864000}{-332659139}$	$\frac{107520}{5056291}$	$\frac{3537}{65536}$
9	$\frac{507317}{28901376}$	$\frac{7526400}{4741632000}$	$\frac{49360000}{604800000}$	$\frac{37324800}{373248000}$	$\frac{24883200}{-102469631}$	$\frac{110592000}{725760000}$	$\frac{15052800}{4741632000}$	$\frac{65536}{11705987}$

These coefficients describe the Hill variation orbit family which is one particular solution to the Hill equations describing the moon's motion [16]. The coefficients presented in Tables 1 and 2 were derived based on the method presented by Wintner [38], and are modified slightly from the form presented by Olikara and Scheeres [22]. We compute the coefficients up to a maximum order $P = 9$, so b_n must be determined for integers $|n| \leq N = 4$ excluding $n = 0$. Note $c_{n,p} = 0$ for $p < 2$.

In order to evaluate the equations of motion in (5), expressions for ∇V , $[A]$, and $[C]$ are needed. Note that $\nabla V = V_{\mathbf{r}} = \frac{\partial V}{\partial \mathbf{r}}$, $[\nabla \nabla V] = V_{\mathbf{r}\mathbf{r}} = \frac{\partial}{\partial \mathbf{r}} \frac{\partial V}{\partial \mathbf{r}}$, $V_{\mathbf{r}m} = \frac{\partial}{\partial m} \frac{\partial V}{\partial \mathbf{r}}$, and $V_{\mathbf{r}\mu} = \frac{\partial}{\partial \mu} \frac{\partial V}{\partial \mathbf{r}}$.

$$(17a) \quad \nabla V = \begin{bmatrix} \left(1 + 2m + \frac{3}{2}m^2\right)x + \frac{3}{2}m^2(x \cos 2\tau - y \sin 2\tau) \\ \left(1 + 2m + \frac{3}{2}m^2\right)y - \frac{3}{2}m^2(y \cos 2\tau + x \sin 2\tau) \\ -m^2z \end{bmatrix} - \frac{m^2}{a_0^3} \left(\frac{1-\mu}{R_{1-\mu}^3} \mathbf{R}_{1-\mu} + \frac{\mu}{R_\mu^3} \mathbf{R}_\mu \right)$$

$$(17b) \quad [A] = \begin{bmatrix} [0_{3 \times 3}] & [I_{3 \times 3}] \\ [\nabla \nabla V] & 2(1+m)[S] \end{bmatrix} \text{ where } [S] = \begin{bmatrix} 0 & 1 & 0 \\ -1 & 0 & 0 \\ 0 & 0 & 0 \end{bmatrix} \text{ if } \boldsymbol{\Omega} = \hat{\mathbf{k}}$$

$$(17c) \quad [C] = \begin{bmatrix} [0_{3 \times 1}] & [0_{3 \times 1}] \\ -2\boldsymbol{\Omega} \times \mathbf{r}' + V_{\mathbf{r}m} & V_{\mathbf{r}\mu} \end{bmatrix}$$

In order to evaluate (17b) and (17c), expressions for $[\nabla \nabla V]$, $V_{\mathbf{r}m}$, and $V_{\mathbf{r}\mu}$ are needed.

$$(18a) \quad [\nabla \nabla V] = \begin{bmatrix} 1 + 2m + \frac{3}{2}m^2(1 + \cos 2\tau) & -\frac{3}{2}m^2 \sin 2\tau & 0 \\ -\frac{3}{2}m^2 \sin 2\tau & 1 + 2m + \frac{3}{2}m^2(1 - \cos 2\tau) & 0 \\ 0 & 0 & -m^2 \end{bmatrix} - \frac{m^2}{a_0^3} \left(\frac{1-\mu}{R_{1-\mu}^3} + \frac{\mu}{R_\mu^3} \right) [I_{3 \times 3}] + 3 \frac{m^2}{a_0^3} \frac{1-\mu}{R_{1-\mu}^5} \mathbf{R}_{1-\mu} \mathbf{R}_{1-\mu}^T + 3 \frac{m^2}{a_0^3} \frac{\mu}{R_\mu^5} \mathbf{R}_\mu \mathbf{R}_\mu^T$$

$$(18b) \quad V_{\mathbf{r}m} = \begin{bmatrix} (2+3m)x + 3m(x \cos 2\tau - y \sin 2\tau) \\ (2+3m)y - 3m(y \cos 2\tau + x \sin 2\tau) \\ -2mz \end{bmatrix} + \frac{m^2}{a_0^3} \frac{(1-\mu)\mu}{R_{1-\mu}^3 R_\mu^3} (R_{1-\mu}^3 - R_\mu^3) \frac{\partial \bar{\boldsymbol{\rho}}}{\partial m} + \frac{m}{a_0^4} \frac{1-\mu}{R_{1-\mu}^4} \left(3ma_0 \frac{\partial R_{1-\mu}}{\partial m} - 2a_0 R_{1-\mu} + 3m R_{1-\mu} \frac{\partial a_0}{\partial m} \right) \mathbf{R}_{1-\mu} + \frac{m}{a_0^4} \frac{\mu}{R_\mu^4} \left(3ma_0 \frac{\partial R_\mu}{\partial m} - 2a_0 R_\mu + 3m R_\mu \frac{\partial a_0}{\partial m} \right) \mathbf{R}_\mu$$

$$(18c) \quad V_{\mathbf{r}\mu} = \frac{m^2}{a_0^3} \frac{1}{R_{1-\mu}^4} \left(R_{1-\mu} + 3(1-\mu) \frac{\partial R_{1-\mu}}{\partial \mu} \right) \mathbf{R}_{1-\mu} + \frac{m^2}{a_0^3} \frac{1}{R_\mu^4} \left(-R_\mu + 3\mu \frac{\partial R_\mu}{\partial \mu} \right) \mathbf{R}_\mu - \frac{m^2}{a_0^3} \left(\frac{1-\mu}{R_{1-\mu}^3} + \frac{\mu}{R_\mu^3} \right) (\bar{\boldsymbol{\rho}} + \hat{\mathbf{i}}_m)$$

The terms needed to evaluate (18) are $\frac{\partial \bar{\boldsymbol{\rho}}}{\partial m}$, $\frac{\partial a_0}{\partial m}$, $\frac{\partial R_{1-\mu}}{\partial m}$, $\frac{\partial R_\mu}{\partial m}$, $\frac{\partial R_{1-\mu}}{\partial \mu}$, and $\frac{\partial R_\mu}{\partial \mu}$. Expressions for all of these terms except $\frac{\partial a_0}{\partial m}$ are presented in (19).

$$(19a) \quad \frac{\partial \bar{\boldsymbol{\rho}}}{\partial m} = \begin{bmatrix} \sum_{n=1}^N \left(\frac{\partial b_n}{\partial m} + \frac{\partial b_{-n}}{\partial m} \right) \cos 2n\tau \\ \sum_{n=1}^N \left(\frac{\partial b_n}{\partial m} - \frac{\partial b_{-n}}{\partial m} \right) \sin 2n\tau \\ 0 \end{bmatrix}$$

$$(19b) \quad \frac{\partial R_{1-\mu}}{\partial m} = \frac{\mu}{R_{1-\mu}} \mathbf{R}_{1-\mu}^T \frac{\partial \bar{\boldsymbol{\rho}}}{\partial m}$$

$$(19c) \quad \frac{\partial R_\mu}{\partial m} = -\frac{1-\mu}{R_\mu} \mathbf{R}_\mu^T \frac{\partial \bar{\boldsymbol{\rho}}}{\partial m}$$

$$(19d) \quad \frac{\partial R_{1-\mu}}{\partial \mu} = \frac{1}{R_{1-\mu}} \mathbf{R}_{1-\mu}^T (\hat{\mathbf{i}}_m + \bar{\boldsymbol{\rho}})$$

$$(19e) \quad \frac{\partial R_\mu}{\partial \mu} = \frac{1}{R_\mu} \mathbf{R}_\mu^T (\hat{\mathbf{i}}_m + \bar{\boldsymbol{\rho}})$$

The final terms needed to evaluate the complete equations of motion are $\frac{\partial a_0}{\partial m}$ and $\frac{\partial b_n}{\partial m}$.

$$(20a) \quad \frac{\partial a_0}{\partial m} = \frac{\partial g_0}{\partial M} \frac{\partial M}{\partial m} \sum_{p=0}^P d_p M^p + g_0 \frac{\partial M}{\partial m} \sum_{p=1}^P p d_p M^{p-1}$$

$$(20b) \quad \frac{\partial b_n}{\partial m} = \frac{\partial M}{\partial m} \sum_{p=1}^P p c_{n,p} M^{p-1}$$

$$(20c) \quad \frac{\partial g_0}{\partial M} = \frac{2}{3} M^{-1/3}$$

$$(20d) \quad \frac{\partial M}{\partial m} = \left(1 - \frac{m}{3}\right)^{-2}$$

B Melnikov Theory Applications with the HR4BP

B.1 Introduction to Melnikov Theory

We will now discuss the derivation of the specific form of the Melnikov-like function presented by Cenedese and Haller [34]. Let the acceleration of an autonomous system be $\mathbf{r}'' = \mathbf{f}(\mathbf{X})$, the flow of the vector field in this autonomous system be defined as $\mathbf{X}(\tau) = \varphi(\mathbf{X}_0, \tau)$, and a small time-periodic perturbation be represented by $\varepsilon \mathbf{g}(\mathbf{X}, \tau_0 + \tau; T_g, \varepsilon)$ where $\mathbf{g}(\mathbf{X}, \tau_0 + \tau; T_g, \varepsilon) = \mathbf{g}(\mathbf{X}, \tau_0 + \tau + T_g; T_g, \varepsilon)$. Let $\mathbf{X}(\tau_0 + \tau; \mathbf{X}_0, T_g, \varepsilon)$ correspond to a trajectory in the perturbed system starting at state \mathbf{X}_0 at time τ_0 .

Let \mathbf{X}_s be a state on a periodic orbit in the unperturbed system with a period T^* that satisfies $bT_g \approx aT^*$ where a and b are relatively prime integers. The state ${}^*\mathbf{X}(s) = \varphi({}^*\mathbf{X}_s, s)$ for any $s \in [0, T^*)$ could be used as the initial state to generate a state time history of the orbit. For a particular value of s , the periodic orbit state time history in the unperturbed system can be represented as ${}^*\mathbf{X}(s + \tau) = \varphi({}^*\mathbf{X}_s, s + \tau)$ for $\tau \in [0, T^*)$ where ${}^*\mathbf{X}(s + \tau) = {}^*\mathbf{X}(s + \tau + T^*)$ and $s \in [0, T^*)$. Say we set a particular value of s and τ_0 and, for a small enough ε , there is a periodic orbit that exists in the slightly perturbed system that corresponds to the unperturbed periodic orbit. Let us assume that the period of this orbit is $T = bT_g = aT^* + \delta T$ where $\delta T = \mathcal{O}(\varepsilon)$. Let us also assume the initial state on this periodic orbit at τ_0 is $\mathbf{X}_0 = {}^*\mathbf{X}(s) + \delta \mathbf{X}_0$ where $\delta \mathbf{X}_0 = \mathcal{O}(\varepsilon)$. For conciseness we will represent $\mathbf{X}(\tau_0 + \tau; \mathbf{X}_0, T_g, \varepsilon)$ as $\mathbf{X}(\tau_0 + \tau; s)$, $\mathbf{g}(\mathbf{X}, \tau_0 + \tau; T_g, \varepsilon)$ as $\mathbf{g}(\mathbf{X}, \tau_0 + \tau)$, and $\tau_0 + \tau$ as α . Define ${}^\varepsilon \delta \mathbf{X}(\tau_0 + \tau) = \mathbf{X}(\tau_0 + \tau; s) - {}^*\mathbf{X}(s + \tau)$ and note ${}^\varepsilon \delta \mathbf{X}(0) = \delta \mathbf{X}_0$. Consider the work done on the perturbed orbit by the perturbing force:

$$(21a)$$

$$\delta W_P(\alpha) = \varepsilon \mathbf{g}(\mathbf{X}(\alpha), \alpha) \cdot \mathbf{r}'(\alpha) d\tau$$

$$(21b) \quad = \varepsilon \left(\mathbf{g}({}^*\mathbf{X}(s + \tau), \alpha) + \left. \frac{\partial \mathbf{g}}{\partial \mathbf{X}} \right|_{{}^*\mathbf{X}(s + \tau), \alpha} {}^\varepsilon \delta \mathbf{X}(\alpha) + \dots \right) \cdot ({}^*\mathbf{r}'(s + \tau) + {}^\varepsilon \delta \mathbf{r}'(\alpha)) d\tau$$

$$(21c) \quad = \varepsilon \mathbf{g}({}^*\mathbf{X}(s + \tau), \alpha) \cdot {}^*\mathbf{r}'(s + \tau) d\tau + \varepsilon \mathbf{g}({}^*\mathbf{X}(s + \tau), \alpha) \cdot {}^\varepsilon \delta \mathbf{r}'(\alpha) d\tau$$

$$+ \varepsilon \left(\left. \frac{\partial \mathbf{g}}{\partial \mathbf{X}} \right|_{{}^*\mathbf{X}(s + \tau), \alpha} {}^\varepsilon \delta \mathbf{X}(\alpha) \right) \cdot {}^*\mathbf{r}'(s + \tau) d\tau$$

$$+ \varepsilon \left(\left. \frac{\partial \mathbf{g}}{\partial \mathbf{X}} \right|_{{}^*\mathbf{X}(s + \tau), \alpha} {}^\varepsilon \delta \mathbf{X}(\alpha) \right) \cdot {}^\varepsilon \delta \mathbf{r}'(\alpha) d\tau + \dots$$

Noting the assumption $\delta \mathbf{X}_0 = \mathcal{O}(\varepsilon)$, we expect the work done over the orbit related to all terms, except the first, in (21c) to produce results that are $\mathcal{O}(\varepsilon^2)$ or higher.

$$(22a) \quad W_P = \int_0^T \delta W_P(\alpha) \, d\tau$$

$$(22b) \quad = \varepsilon \int_0^{aT^* + \delta T} \mathbf{g}(*\mathbf{X}(s + \tau), \alpha) \cdot *\mathbf{r}'(s + \tau) \, d\tau + \mathcal{O}(\varepsilon^2)$$

$$(22c) \quad = \varepsilon \int_0^{aT^*} \mathbf{g}(*\mathbf{X}(s + \tau), \tau_0 + \tau) \cdot *\mathbf{r}'(s + \tau) \, d\tau + \mathcal{O}(\varepsilon^2)$$

The previous equation is the Taylor series expansion of the so-called energy function. In this work, we refer to the leading order term of the Taylor series expansion of the energy function as the Melnikov function [34]. Simplified expressions for the Melnikov function are provided in the following equation.

$$(23a) \quad \mathcal{M}(s, \tau_0) = \int_0^{aT^*} \mathbf{g}(*\mathbf{X}(s + \tau), \tau_0 + \tau) \cdot *\mathbf{r}'(s + \tau) \, d\tau$$

$$(23b) \quad = \sum_{k=0}^{a-1} \left[\int_0^{T^*} \mathbf{g}(*\mathbf{X}(s + \tau), \tau_0 + kT^* + \tau) \cdot *\mathbf{r}'(s + \tau) \, d\tau \right]$$

For an orbit to be a periodic solution, there must be no work done by the non-conservative forces on the orbit over one period. The zeros of the Melnikov function represent where this is the case when considering the leading order terms. We expect (resonant) periodic orbits from the unperturbed system will continue into the perturbed system at points where $\mathcal{M}(s, \tau_0) = 0$, where τ_0 is the initial time of integration in the perturbed system. In the case where $\mathcal{M}(s, \tau_0) \equiv 0$ identically, a higher-order analysis is required. Before we present proofs of the three propositions, it is useful to note that $*\mathbf{X}(s + \tau + kT^*) = *\mathbf{X}(s + \tau)$ for any integer k (i.e., $k \in \mathbb{Z}$) and $\mathbf{g}(*\mathbf{X}(s + \tau + aT^*), \tau_0 + \tau + aT^*) = \mathbf{g}(*\mathbf{X}(s + \tau), \tau_0 + \tau)$.

Proof (Proof of Proposition 1). These results can be derived explicitly from computations. Beginning with the left-hand side of Proposition 1(a), we separate the integral into two terms using linearity:

$$(24a) \quad \mathcal{M}(s + \tau_s, \tau_0 + \tau_s) = \sum_{k=0}^{a-1} \left[\int_0^{T^*} \mathbf{g}(*\mathbf{X}(s + \tau_s + \tau), \tau_0 + \tau_s + kT^* + \tau) \cdot *\mathbf{r}'(s + \tau_s + \tau) \, d\tau \right]$$

$$(24b) \quad = \sum_{k=0}^{a-1} A_k + \sum_{k=0}^{a-1} B_k$$

We then analyze the two terms independently. Note that the product of $*\mathbf{r}'$ and \mathbf{g} (the integrand of (23a)) is periodic with a period of aT^* . Hence, by periodicity, we shift the integration bounds:

$$(25a) \quad \sum_{k=0}^{a-1} A_k = \sum_{k=0}^{a-1} \left[\int_0^{T^* - \tau_s} \mathbf{g}(*\mathbf{X}(s + \tau_s + \tau), \tau_0 + \tau_s + kT^* + \tau) \cdot *\mathbf{r}'(s + \tau_s + \tau) \, d\tau \right]$$

$$(25b) \quad = \sum_{k=0}^{a-1} \left[\int_{\tau_s}^{T^*} \mathbf{g}(*\mathbf{X}(s + \tau), \tau_0 + kT^* + \tau) \cdot *\mathbf{r}'(s + \tau) \, d\tau \right]$$

Applying a similar trick to the summation bounds of the second term, we obtain:

$$\begin{aligned}
(26a) \quad \sum_{k=0}^{a-1} B_k &= \sum_{k=0}^{a-1} \left[\int_{T^* - \tau_s}^{T^*} \mathbf{g}(*\mathbf{X}(s + \tau_s + \tau), \tau_0 + \tau_s + kT^* + \tau) \cdot * \mathbf{r}'(s + \tau_s + \tau) \, d\tau \right] \\
(26b) \quad &= \sum_{k=0}^{a-1} \left[\int_0^{\tau_s} \mathbf{g}(*\mathbf{X}(s + \tau), \tau_0 + (k+1)T^* + \tau) \cdot * \mathbf{r}'(s + \tau) \, d\tau \right] \\
(26c) \quad &= \sum_{k=1}^a \left[\int_0^{\tau_s} \mathbf{g}(*\mathbf{X}(s + \tau), \tau_0 + kT^* + \tau) \cdot * \mathbf{r}'(s + \tau) \, d\tau \right] \\
(26d) \quad &= \sum_{k=1}^{a-1} \left[\int_0^{\tau_s} \mathbf{g}(*\mathbf{X}(s + \tau), \tau_0 + kT^* + \tau) \cdot * \mathbf{r}'(s + \tau) \, d\tau \right] \\
&\quad + \left[\int_0^{\tau_s} \mathbf{g}(*\mathbf{X}(s + \tau), \tau_0 + aT^* + \tau) \cdot * \mathbf{r}'(s + \tau) \, d\tau \right] \\
(26e) \quad &= \sum_{k=1}^{a-1} \left[\int_0^{\tau_s} \mathbf{g}(*\mathbf{X}(s + \tau), \tau_0 + kT^* + \tau) \cdot * \mathbf{r}'(s + \tau) \, d\tau \right] \\
&\quad + \left[\int_0^{\tau_s} \mathbf{g}(*\mathbf{X}(s + \tau), \tau_0 + \tau) \cdot * \mathbf{r}'(s + \tau) \, d\tau \right] \\
(26f) \quad &= \sum_{k=0}^{a-1} \left[\int_0^{\tau_s} \mathbf{g}(*\mathbf{X}(s + \tau), \tau_0 + kT^* + \tau) \cdot * \mathbf{r}'(s + \tau) \, d\tau \right]
\end{aligned}$$

Substituting these simplified expressions back into the summation for $\mathcal{M}(s + \tau_s, \tau_0 + \tau_s)$ shows:

$$\begin{aligned}
(27a) \quad \mathcal{M}(s + \tau_s, \tau_0 + \tau_s) &= \sum_{k=0}^{a-1} \left[\int_{\tau_s}^{T^*} \mathbf{g}(*\mathbf{X}(s + \tau), \tau_0 + kT^* + \tau) \cdot * \mathbf{r}'(s + \tau) \, d\tau \right] \\
&\quad + \sum_{k=0}^{a-1} \left[\int_0^{\tau_s} \mathbf{g}(*\mathbf{X}(s + \tau), \tau_0 + kT^* + \tau) \cdot * \mathbf{r}'(s + \tau) \, d\tau \right] \\
(27b) \quad &= \sum_{k=0}^{a-1} \left[\int_0^{T^*} \mathbf{g}(*\mathbf{X}(s + \tau), \tau_0 + kT^* + \tau) \cdot * \mathbf{r}'(s + \tau) \, d\tau \right] \\
(27c) \quad &= \mathcal{M}(s, \tau_0)
\end{aligned}$$

Hence, Proposition 1(a) is proved. To prove Proposition 1(b), we again use the periodicity of \mathbf{g} , shifting the integration bounds and separating into two terms by linearity.

$$\begin{aligned}
(28a) \quad \mathcal{M}(s + \tau_s, \tau_0) &= \int_0^{aT^*} \mathbf{g}(*\mathbf{X}(s + \tau_s + \tau), \tau_0 + \tau) \cdot * \mathbf{r}'(s + \tau_s + \tau) \, d\tau \\
(28b) \quad &= \int_{\tau_s}^{aT^* + \tau_s} \mathbf{g}(*\mathbf{X}(s + \tau), \tau_0 - \tau_s + \tau) \cdot * \mathbf{r}'(s + \tau) \, d\tau \\
(28c) \quad &= \int_{\tau_s}^{aT^*} \mathbf{g}(*\mathbf{X}(s + \tau), \tau_0 - \tau_s + \tau) \cdot * \mathbf{r}'(s + \tau) \, d\tau \\
&\quad + \int_0^{\tau_s} \mathbf{g}(*\mathbf{X}(s + \tau), \tau_0 - \tau_s + \tau) \cdot * \mathbf{r}'(s + \tau) \, d\tau \\
(28d) \quad &= \int_0^{aT^*} \mathbf{g}(*\mathbf{X}(s + \tau), \tau_0 - \tau_s + \tau) \cdot * \mathbf{r}'(s + \tau) \, d\tau \\
(28e) \quad &= \mathcal{M}(s, \tau_0 - \tau_s)
\end{aligned}$$

Hence, Proposition 1(b) is proved. ■

B.2 Manipulating the HR4BP Equations of Motion

Recall the definition of the Melnikov function in (11) and the terms \mathbf{h}_2 and $[P]$ in (10). Note that Proposition 2 and Proposition 3 were derived assuming \mathbf{h}_2 is used in (11). For the following proofs, it will be useful to note that $[P]$ does not depend on τ_0 (i.e., think of $[P]$ as $[P(\mathbf{X}(\alpha))]$ which will be replaced by $[P(*\mathbf{X}(s+\tau))]$ when evaluating the Melnikov function). It will also be useful to recall the following trigonometry identities.

$$(29a) \quad \sin(\theta_1 + \theta_2) = \sin(\theta_1)\cos(\theta_2) + \cos(\theta_1)\sin(\theta_2)$$

$$(29b) \quad \cos(\theta_1 + \theta_2) = \cos(\theta_1)\cos(\theta_2) - \sin(\theta_1)\sin(\theta_2)$$

$$(29c) \quad \sin(2\theta) = \cos\left(2\left(\theta - \frac{\pi}{4}\right)\right)$$

$$(29d) \quad \cos(2\theta) = -\sin\left(2\left(\theta - \frac{\pi}{4}\right)\right)$$

Proof (Proof of Proposition 2). The results follow from direct computations. We begin by simplifying the form of \mathbf{h}_2 using the identities given in (29):

$$(30a) \quad \mathbf{h}_2(\mathbf{X}(\alpha), \alpha + \tau_s) = -\frac{3}{2} \begin{bmatrix} -\cos(2\alpha + \tau_s) & \sin(2\alpha + \tau_s) & 0 \\ \sin(2\alpha + \tau_s) & \cos(2\alpha + \tau_s) & 0 \\ 0 & 0 & \frac{2}{3} \end{bmatrix} \mathbf{r}(\alpha) \\ -\frac{1}{8}(1-\mu)\mu [P(\mathbf{X}(\alpha))] \begin{bmatrix} -8\cos(2\alpha + \tau_s) \\ 11\sin(2\alpha + \tau_s) \\ 0 \end{bmatrix}$$

$$(30b) \quad = -\cos(2\tau_s) \frac{3}{2} \begin{bmatrix} -\cos(2\alpha) & \sin(2\alpha) & 0 \\ \sin(2\alpha) & \cos(2\alpha) & 0 \\ 0 & 0 & \frac{2}{3} \end{bmatrix} \mathbf{r}(\alpha) \\ -\sin(2\tau_s) \frac{3}{2} \begin{bmatrix} \sin(2\alpha) & \cos(2\alpha) & 0 \\ \cos(2\alpha) & -\sin(2\alpha) & 0 \\ 0 & 0 & 0 \end{bmatrix} \mathbf{r}(\alpha)$$

$$(30c) \quad -\cos(2\tau_s) \frac{1}{8}(1-\mu)\mu [P(\mathbf{X}(\alpha))] \begin{bmatrix} -8\cos(2\alpha) \\ 11\sin(2\alpha) \\ 0 \end{bmatrix} \\ -\sin(2\tau_s) \frac{1}{8}(1-\mu)\mu [P(\mathbf{X}(\alpha))] \begin{bmatrix} 8\sin(2\alpha) \\ 11\cos(2\alpha) \\ 0 \end{bmatrix} \\ = \cos(2\tau_s) \mathbf{h}_2(\mathbf{X}(\alpha), \alpha) + \sin(2\tau_s) \begin{bmatrix} 0 \\ 0 \\ z(\alpha) \end{bmatrix} - \sin(2\tau_s) \begin{bmatrix} 0 \\ 0 \\ z(\alpha) \end{bmatrix}$$

$$(30d) \quad -\sin(2\tau_s) \frac{3}{2} \begin{bmatrix} \cos\left(2\left(\alpha - \frac{\pi}{4}\right)\right) & -\sin\left(2\left(\alpha - \frac{\pi}{4}\right)\right) & 0 \\ -\sin\left(2\left(\alpha - \frac{\pi}{4}\right)\right) & -\cos\left(2\left(\alpha - \frac{\pi}{4}\right)\right) & 0 \\ 0 & 0 & 0 \end{bmatrix} \mathbf{r}(\alpha) \\ -\sin(2\tau_s) \frac{1}{8}(1-\mu)\mu [P(\mathbf{X}(\alpha))] \begin{bmatrix} 8\cos\left(2\left(\alpha - \frac{\pi}{4}\right)\right) \\ -11\sin\left(2\left(\alpha - \frac{\pi}{4}\right)\right) \\ 0 \end{bmatrix}$$

$$(30d) \quad = \cos(2\tau_s) \mathbf{h}_2(\mathbf{X}(\alpha), \alpha) - \sin(2\tau_s) \mathbf{h}_2\left(\mathbf{X}(\alpha), \alpha - \frac{\pi}{4}\right) \\ - \sin(2\tau_s) z(\alpha) \hat{\mathbf{k}}$$

Substituting the simplified form of \mathbf{h}_2 into the equation for $\mathcal{M}(s, \tau_0 + \tau_s)$, we obtain:

$$\begin{aligned}
(31a) \quad \mathcal{M}(s, \tau_0 + \tau_s) &= \int_0^{aT^*} \mathbf{h}_2({}^* \mathbf{X}(s + \tau), \alpha + \tau_s) \cdot {}^* \mathbf{r}'(s + \tau) \, d\tau \\
(31b) \quad &= \int_0^{aT^*} \cos(2\tau_s) \mathbf{h}_2({}^* \mathbf{X}(s + \tau), \alpha) \cdot {}^* \mathbf{r}'(s + \tau) \, d\tau \\
&\quad + \int_0^{aT^*} -\sin(2\tau_s) \mathbf{h}_2\left({}^* \mathbf{X}(s + \tau), \alpha - \frac{\pi}{4}\right) \cdot {}^* \mathbf{r}'(s + \tau) \, d\tau \\
&\quad + \int_0^{aT^*} -\sin(2\tau_s) {}^* z(s + \tau) \hat{\mathbf{k}} \cdot {}^* \mathbf{r}'(s + \tau) \, d\tau \\
(31c) \quad &= \cos(2\tau_s) \int_0^{aT^*} \mathbf{h}_2({}^* \mathbf{X}(s + \tau), \tau_0 + \tau) \cdot {}^* \mathbf{r}'(s + \tau) \, d\tau \\
&\quad - \sin(2\tau_s) \int_0^{aT^*} \mathbf{h}_2\left({}^* \mathbf{X}(s + \tau), \tau_0 - \frac{\pi}{4} + \tau\right) \cdot {}^* \mathbf{r}'(s + \tau) \, d\tau \\
&\quad - \sin(2\tau_s) \int_0^{aT^*} {}^* z(s + \tau) \cdot {}^* z'(s + \tau) \, d\tau \\
(31d) \quad &= \cos(2\tau_s) \mathcal{M}(s, \tau_0) - \sin(2\tau_s) \mathcal{M}\left(s, \tau_0 - \frac{\pi}{4}\right) - \sin(2\tau_s) (0) \\
(31e) \quad &= \cos(2\tau_s) \mathcal{M}(s, \tau_0) - \sin(2\tau_s) \mathcal{M}\left(s, \tau_0 - \frac{\pi}{4}\right)
\end{aligned}$$

proving Proposition 2(a). Proposition 2(b) follows from an application of Proposition 1(b):

$$\begin{aligned}
(32a) \quad \mathcal{M}(s + \tau_s, \tau_0) &= \mathcal{M}(s, \tau_0 - \tau_s) \\
(32b) \quad &= \cos(-2\tau_s) \mathcal{M}(s, \tau_0) - \sin(-2\tau_s) \mathcal{M}\left(s, \tau_0 - \frac{\pi}{4}\right) \\
(32c) \quad &= \cos(2\tau_s) \mathcal{M}(s, \tau_0) + \sin(2\tau_s) \mathcal{M}\left(s, \tau_0 - \frac{\pi}{4}\right) \\
(32d) \quad &= \cos(2\tau_s) \mathcal{M}(s, \tau_0) + \sin(2\tau_s) \mathcal{M}\left(s + \frac{\pi}{4}, \tau_0\right)
\end{aligned}$$

Hence, Proposition 2(b) is proved. ■

The final proposition we will prove applies to periodic orbits in the CR3BP that exhibit a half-period symmetry condition at some $s \in \mathbb{R}$, which occurs often in the computations and analyses contained in the present article.

Proof (Proof of Proposition 3). We will begin by obtaining a more detailed expression for the $[P]$ matrix presented in (10c). For conciseness we will represent $\mathbf{X}(\alpha)$ as \mathbf{X} .

$$(33a) \quad [P] = \begin{bmatrix} a & -(d(x + \mu) + e)y - (d(x + \mu) + e)z & \\ - (d(x + \mu) + e)y & b & -dyz \\ - (d(x + \mu) + e)z & -dyz & c \end{bmatrix}$$

$$(33b) \quad a = \kappa_3 - 3(x + \mu)^2 \kappa_5 - 3 \frac{2(x + \mu) - 1}{R_{\mu, C}^5}$$

$$(33c) \quad b = \kappa_3 - 3y^2 \kappa_5$$

$$(33d) \quad c = \kappa_3 - 3z^2 \kappa_5$$

$$(33e) \quad d = 3\kappa_5$$

$$(33f) \quad e = \frac{3}{R_{\mu, C}^5}$$

$$(33g) \quad \kappa_k = \frac{1}{R_{1-\mu, C}^k} - \frac{1}{R_{\mu, C}^k}$$

Note the values of a, b, c, d, e, κ_3 , and κ_5 are the same when evaluated at ${}^* \mathbf{X}(s + T^* - \tau)$ and ${}^* \mathbf{X}(s + \tau)$ if the point s satisfies the half-period symmetry conditions presented in (13). We will now use the result in (33a) to obtain another expression for \mathbf{h}_2 , which was presented in (10a).

$$(34) \quad \mathbf{h}_2(\mathbf{X}, \alpha) = \left(\frac{3}{2} \begin{bmatrix} x \\ -y \\ 0 \end{bmatrix} - (1 - \mu) \mu \begin{bmatrix} -a \\ y(d(x + \mu) + e) \\ z(d(x + \mu) + e) \end{bmatrix} \right) \cos(2\alpha) \\ + \left(\frac{3}{2} \begin{bmatrix} -y \\ -x \\ 0 \end{bmatrix} + \frac{11}{8} (1 - \mu) \mu \begin{bmatrix} y(d(x + \mu) + e) \\ -b \\ dyz \end{bmatrix} \right) \sin(2\alpha) + \begin{bmatrix} 0 \\ 0 \\ -z \end{bmatrix}$$

Evaluating the dot product of \mathbf{h}_2 with the velocity \mathbf{r}' yields:

$$(35a) \quad \mathbf{h}_2(\mathbf{X}, \alpha) \cdot \mathbf{r}' = J(\mathbf{X}) \cos(2\alpha) + K(\mathbf{X}) \sin(2\alpha) - zz'$$

$$(35b) \quad J(\mathbf{X}) = \frac{3}{2} (xx' - yy') - (1 - \mu) \mu (-ax' + (yy' + zz')(d(x + \mu) + e))$$

$$(35c) \quad K(\mathbf{X}) = \frac{3}{2} (-yx' - xy') + \frac{11}{8} (1 - \mu) \mu (yx'(d(x + \mu) + e) - by' + dyzz')$$

Note that $J({}^* \mathbf{X}(s + T^* - \tau)) = -J({}^* \mathbf{X}(s + \tau))$ and $K({}^* \mathbf{X}(s + T^* - \tau)) = K({}^* \mathbf{X}(s + \tau))$ if the point corresponding to s satisfies the half-period symmetry conditions presented in (13). Note a u substitution is performed on the second integral between (36b) and (36c) where $u = T^* - \tau$. The variable τ is still used instead of u as the name of the variable is arbitrary.

$$(36a) \quad \mathcal{M}(s, \tau_0) = \sum_{k=0}^{a-1} \left[\int_0^{T^*} \mathbf{h}_2({}^* \mathbf{X}(s + \tau), \tau_0 + kT^* + \tau) \cdot {}^* \mathbf{r}'(s + \tau) \, d\tau \right]$$

$$(36b) \quad = \sum_{k=0}^{a-1} \left[\int_0^{T^*/2} \mathbf{h}_2({}^* \mathbf{X}(s + \tau), \tau_0 + kT^* + \tau) \cdot {}^* \mathbf{r}'(s + \tau) \, d\tau \right] \\ + \sum_{k=0}^{a-1} \left[- \int_{T^*}^{T^*/2} \mathbf{h}_2({}^* \mathbf{X}(s + \tau), \tau_0 + kT^* + \tau) \cdot {}^* \mathbf{r}'(s + \tau) \, d\tau \right]$$

$$(36c) \quad = \sum_{k=0}^{a-1} \left[\int_0^{T^*/2} \mathbf{h}_2({}^* \mathbf{X}(s + \tau), \tau_0 + kT^* + \tau) \cdot {}^* \mathbf{r}'(s + \tau) \, d\tau \right] \\ + \sum_{k=0}^{a-1} \left[\int_0^{T^*/2} \mathbf{h}_2({}^* \mathbf{X}(s + T^* - \tau), \tau_0 + (k+1)T^* - \tau) \cdot {}^* \mathbf{r}'(s + T^* - \tau) \, d\tau \right]$$

$$(36d) \quad = \sum_{k=0}^{a-1} \left[\int_0^{T^*/2} J({}^* \mathbf{X}(s + \tau)) \cos(2(\tau_0 + kT^* + \tau)) \, d\tau \right. \\ + \int_0^{T^*/2} K({}^* \mathbf{X}(s + \tau)) \sin(2(\tau_0 + kT^* + \tau)) \, d\tau \\ \left. - \int_0^{T^*/2} {}^* z(s + \tau) {}^* z'(s + \tau) \, d\tau \right] \\ + \sum_{k=0}^{a-1} \left[\int_0^{T^*/2} J({}^* \mathbf{X}(s + T^* - \tau)) \cos(2(\tau_0 + (k+1)T^* - \tau)) \, d\tau \right. \\ + \int_0^{T^*/2} K({}^* \mathbf{X}(s + T^* - \tau)) \sin(2(\tau_0 + (k+1)T^* - \tau)) \, d\tau \\ \left. - \int_0^{T^*/2} {}^* z(s + T^* - \tau) {}^* z'(s + T^* - \tau) \, d\tau \right]$$

(37a)

$$\mathcal{M}(s, \tau_0) = \sum_{k=0}^{a-1} [C_k] + \sum_{k=0}^{a-1} [D_k]$$

$$(37b) \quad C_k = \int_0^{T^*/2} J(*\mathbf{X}(s + \tau)) (\cos(2(\tau_0 + kT^* + \tau)) - \cos(2(\tau_0 + (k+1)T^* - \tau))) d\tau$$

$$(37c) \quad D_k = \int_0^{T^*/2} K(*\mathbf{X}(s + \tau)) (\sin(2(\tau_0 + kT^* + \tau)) + \sin(2(\tau_0 + (k+1)T^* - \tau))) d\tau$$

We seek to evaluate both of the terms in (37), though we first develop expressions for some intermediate terms. Recall aT^* must be an integer multiple of π as $T_g = \pi$. Note that from trigonometry identities:

$$(38a) \quad \sin(2(\tau_0 + kT^* + \tau)) + \sin(2(\tau_0 + kT^* - \tau)) = 2 \sin(2(\tau_0 + kT^*)) \cos(2\tau)$$

$$(38b) \quad \cos(2(\tau_0 + kT^* + \tau)) - \cos(2(\tau_0 + kT^* - \tau)) = -2 \sin(2(\tau_0 + kT^*)) \sin(2\tau)$$

$$(38c) \quad \begin{aligned} \sin(2(\tau_0 + \tau)) + \sin(2(\tau_0 + aT^* - \tau)) &= 2 \sin(2\tau_0 + aT^*) \cos(-aT^* + 2\tau) \\ &= 2 \sin(2\tau_0) \cos(2\tau) \end{aligned}$$

$$(38d) \quad \begin{aligned} \cos(2(\tau_0 + \tau)) - \cos(2(\tau_0 + aT^* - \tau)) &= -2 \sin(2\tau_0 + aT^*) \sin(-aT^* + 2\tau) \\ &= -2 \sin(2\tau_0) \sin(2\tau) \end{aligned}$$

With psychic foresight we will present the following two equations. Equations (39) and (40) are related to the terms in C_k and D_k , respectively.

$$(39a) \quad \sum_{k=0}^{a-1} [\cos(2(\tau_0 + kT^* + \tau)) - \cos(2(\tau_0 + (k+1)T^* - \tau))] = \cos(2(\tau_0 + 0 + \tau))$$

$$(39b) \quad \begin{aligned} &+ \sum_{k=1}^{a-1} [\cos(2(\tau_0 + kT^* + \tau)) - \cos(2(\tau_0 + kT^* - \tau))] \\ &- \cos(2(\tau_0 + aT^* - \tau)) \\ &= -2 \sin(2\tau_0) \sin(2\tau) - \sum_{k=1}^{a-1} [2 \sin(2(\tau_0 + kT^*)) \sin(2\tau)] \end{aligned}$$

$$(39c) \quad = -2 \sin(2\tau) \sum_{k=0}^{a-1} [\sin(2(\tau_0 + kT^*))]$$

$$(40a) \quad \sum_{k=0}^{a-1} [\sin(2(\tau_0 + kT^* + \tau)) + \sin(2(\tau_0 + (k+1)T^* - \tau))] = \sin(2(\tau_0 + 0 + \tau))$$

$$(40b) \quad \begin{aligned} &+ \sum_{k=1}^{a-1} [\sin(2(\tau_0 + kT^* + \tau)) + \sin(2(\tau_0 + kT^* - \tau))] \\ &+ \sin(2(\tau_0 + aT^* - \tau)) \\ &= 2 \sin(2\tau_0) \cos(2\tau) + \sum_{k=1}^{a-1} [2 \sin(2(\tau_0 + kT^*)) \cos(2\tau)] \end{aligned}$$

$$(40c) \quad = 2 \cos(2\tau) \sum_{k=0}^{a-1} [\sin(2(\tau_0 + kT^*))]$$

Substituting the result in (39) back into (37b) yields:

$$(41a) \quad \sum_{k=0}^{a-1} [C_k] = \int_0^{T^*/2} J(*\mathbf{X}(s+\tau)) \left(-2 \sin(2\tau) \sum_{k=0}^{a-1} [\sin(2(\tau_0 + kT^*))] \right) d\tau$$

$$(41b) \quad = 2 \left(\sum_{k=0}^{a-1} [\sin(2(\tau_0 + kT^*))] \right) \int_0^{T^*/2} -J(*\mathbf{X}(s+\tau)) \sin(2\tau) d\tau$$

Substituting the result in (40) back into (37c) yields:

$$(42a) \quad \sum_{k=0}^{a-1} [D_k] = \int_0^{T^*/2} K(*\mathbf{X}(s+\tau)) \left(2 \cos(2\tau) \sum_{k=0}^{a-1} [\sin(2(\tau_0 + kT^*))] \right) d\tau$$

$$(42b) \quad = 2 \left(\sum_{k=0}^{a-1} [\sin(2(\tau_0 + kT^*))] \right) \int_0^{T^*/2} K(*\mathbf{X}(s+\tau)) \cos(2\tau) d\tau$$

The result in (12) can be obtained by substituting the expressions from (41) and (42) back into (37) while using the following identity.

$$(43a) \quad \sum_{k=0}^{a-1} [\sin(2(\tau_0 + kT^*))] = \csc(T^*) \sin(aT^*) \sin((a-1)T^* + 2\tau_0)$$

$$(43b) \quad = \begin{cases} \sin(2\tau_0), & \text{if } a = 1 \\ 0, & \text{otherwise} \end{cases} \quad \blacksquare$$

If \mathbf{h}_3 had been used instead of \mathbf{h}_2 the same results shown in Proposition 2 and Proposition 3 would be obtained except:

$$(44a) \quad \mathbf{h}_3(\mathbf{X}, \alpha) \cdot \mathbf{r}' = J(\mathbf{X}) \cos(2\alpha) + K(\mathbf{X}) \sin(2\alpha) + 0$$

$$(44b) \quad J(\mathbf{X}) = -\frac{38}{12} (1-\mu) \mu (-ax' + (yy' + zz')(d(x+\mu) + e))$$

$$(44c) \quad K(\mathbf{X}) = \frac{59}{12} (1-\mu) \mu (yx'(d(x+\mu) + e) - by' + dyzz')$$

While there are likely additional results relating to the Melnikov function that could be identified, however, the main results relevant to the analysis in this work—continuing CR3BP periodic orbits into the HR4BP—are presented and proved in the three Propositions of this appendix.

References

- [1] NASA Office of the Chief Financial Officer: NASA Strategic Plan 2022. N PD 1001 0D, NASA (Mar 2022)
- [2] Whitley, R.J., Davis, D.C., Burke, L.M., McCarthy, B.P., Power, R.J., McGuire, M.L., Howell, K.C.: Earth-Moon Near Rectilinear Halo and Butterfly Orbits for Lunar Surface Exploration. In: AAS/AIAA Astrodynamics Conference (2018)
- [3] Szebehely, V.: Theory of Orbits: The Restricted Problem of Three Bodies. Academic Press Inc (1967)
- [4] Park, B., Howell, K.C.: Leveraging Intermediate Dynamical Models for Transitioning from the Circular Restricted Three-Body Problem to an Ephemeris Model. In: AAS/AIAA Astrodynamics Specialist Conference (2022)
- [5] Peng, H., Bai, X.: Natural deep space satellite constellation in the Earth-Moon elliptic system. *Acta Astronautica* **153**, 240–258 (2018)
- [6] Huang, S.-S.: Very Restricted Four-Body Problem. TN D-501, NASA (Sep 1960)
- [7] Gómez, G., Jorba, Á., Masdemont, J., Simó, C.: Normal form of the bicircular model and related topics. In: Dynamics and Mission Design Near Libration Points, pp. 53–110. World Scientific (2001)
- [8] Rosales, J.J.: On the effect of the Sun’s gravity around the Earth-Moon L1 and L2 libration points. PhD thesis, Universitat de Barcelona (2020)
- [9] Jorba-Cuscó, M., Farrés, A., Jorba, Á.: Two Periodic Models for the Earth-Moon System. *Frontiers in Applied Mathematics and Statistics* **4** (2018)
- [10] Simó, C., Gómez, G., Jorba, Á., Masdemont, J.: The Bicircular Model Near the Triangular Libration Points of the RTBP. In: From Newton to Chaos: Modern Techniques for Understanding and Coping with Chaos in N-Body Dynamical Systems, pp. 343–370. Springer (1995)
- [11] Boudad, K.K., Howell, K.C., Davis, D.C.: Dynamics of synodic resonant near rectilinear halo orbits in the bicircular four-body problem. *Advances in Space Research* **66**(9), 2194–2214 (2020)
- [12] Castellá, E., Jorba, Á.: On the vertical families of two-dimensional tori near the triangular points of the Bicircular problem. *Celestial Mechanics and Dynamical Astronomy* **76**, 35–54 (2000)
- [13] Rosales, J.J., Jorba, Á., Jorba-Cuscó, M.: Families of Halo-like invariant tori around L2 in the Earth-Moon Bicircular Problem. *Celestial Mechanics and Dynamical Astronomy* **133** (2021)
- [14] Andreu, M.A.: The Quasi-bicircular Problem. PhD thesis, Universitat de Barcelona (1998)
- [15] Rosales, J.J., Jorba, Á., Jorba-Cuscó, M.: Invariant manifolds near L1 and L2 in the quasi-bicircular problem. *Celestial Mechanics and Dynamical Astronomy* **135** (2023)
- [16] Scheeres, D.J.: The Restricted Hill Four-Body Problem with Applications to the Earth–Moon–Sun System. *Celestial Mechanics and Dynamical Astronomy* **70**(2), 75–98 (1998)
- [17] Peterson, L.T., Rosales, J.J., Scheeres, D.J.: The vicinity of Earth–Moon L1 and L2 in the Hill restricted 4-body problem. *Physica D: Nonlinear Phenomena* **455** (2023)

- [18] Olikara, Z.P., Gómez, G., Masdemont, J.J.: A Note on Dynamics About the Coherent Sun-Earth-Moon Collinear Libration Points. In: Gómez, G., Masdemont, J.J. (eds.) *Astrodynamics Network AstroNet-II*, pp. 183–192. Springer (2016)
- [19] Henry, D., Rosales, J., Brown, G., Peterson, L., Scheeres, D.: Quasi-Periodic Orbits near Earth-Moon L1 in the Hill Restricted Four-Body Problem. In: *34th ISTS* (2023)
- [20] Henry, D.B., Rosales, J., Brown, G.M., Scheeres, D.J.: Quasi-Periodic Orbits near Earth-Moon L1 and L2 in the Hill Restricted Four-Body Problem. In: *AAS/AIAA Astrodynamics Specialist Conference* (2023)
- [21] Peterson, L.T., Jorba, A., Brown, G.M., Scheeres, D.J.: Dynamics Around the Earth-Moon Triangular Points in the Hill Restricted 4-Body Problem. *Communications in Nonlinear Science and Numerical Simulation* (2024). In Preparation
- [22] Olikara, Z.P., Scheeres, D.J.: Mapping Connections Between Planar Sun-Earth-Moon Libration Orbits. In: *27th AAS/AIAA Space Flight Mechanics Meeting* (2017)
- [23] Sanaga, R.R., Howell, K.C.: Synodic Resonant Halo Orbits in the Hill Restricted Four-Body Problem. In: *33rd AAS/AIAA Space Flight Mechanics Meeting* (2023)
- [24] Melnikov, V.K.: On the stability of the center for time periodic perturbations. *Transactions of the Moscow Mathematical Society* **12**, 1–57 (1963)
- [25] Greenspan, B.D., Holmes, P.: *Homoclinic Orbits, Subharmonics and Global Bifurcations in Forced Oscillations*. ADA103564, U.S. Army Research Office (Jun 1981)
- [26] Wiggins, S.: *Introduction to Applied Nonlinear Dynamical Systems and Chaos*, 2nd edn. *Texts in Applied Mathematics*. Springer (2003)
- [27] Guckenheimer, J., Holmes, P.: *Nonlinear Dynamical Systems, and Bifurcations of Vector Fields*. *Applied Mathematical Sciences*. Springer (1983)
- [28] Perko, L.: *Differential Equations and Dynamical Systems*, 3rd edn. *Texts in Applied Mathematics*. Springer (2001)
- [29] Haller, G.: *Chaos Near Resonance*. *Applied Mathematical Sciences*. Springer (1999)
- [30] Guo, X., Tian, R., Xue, Q., Zhang, X.: Sub-harmonic Melnikov function for a high-dimensional non-smooth coupled system. *Chaos, Solitons & Fractals* **164** (2022)
- [31] Veerman, P., Holmes, P.: The existence of arbitrarily many distinct periodic orbits in a two degree of freedom hamiltonian system. *Physica D: Nonlinear Phenomena* **14**(2), 177–192 (1985)
- [32] Yagasaki, K.: The melnikov theory for subharmonics and their bifurcations in forced oscillations. *SIAM Journal on Applied Mathematics* **56**(6), 1720–1765 (1996)
- [33] Polcar, L., Semerák, O.: Free motion around black holes with discs or rings: Between integrability and chaos. VI. The Melnikov method. *Phys. Rev. D* **100**(10) (2019)
- [34] Cenedese, M., Haller, G.: How do conservative backbone curves perturb into forced responses? A Melnikov function analysis. *Proceedings of the Royal Society A* **476**(2234) (2020)
- [35] Rhouma, M.B.H., Chicone, C.: On the Continuation of Periodic Orbits. *Methods and Applications of Analysis* **7**(1), 85–104 (2000)
- [36] Scheeres, D.J.: *Orbital Motion in Strongly Perturbed Environments*. Springer (2012)

- [37] Holmes, P.: Poincaré, celestial mechanics, dynamical-systems theory and “chaos”. *Physics Reports* **193**(3), 137–163 (1990)
- [38] Wintner, A.: *The Analytical Foundations of Celestial Mechanics*. Dover Books on Physics. Dover Publications (1952)